Statistical mechanics of directed models of polymers in the square lattice

2003 J. Phys. A: Math. Gen. 36 R11

(http://iopscience.iop.org/0305-4470/36/15/201)

INSTITUTE OF PHYSICS PUBLISHING JOURNAL OF PHYSICS A: MATHEMATICAL AND GENERAL

J. Phys. A: Math. Gen. **36** (2003) R11–R61 PII: S0305-4470(03)52469-6

TOPICAL REVIEW

Statistical mechanics of directed models of polymers in the square lattice

E J Janse van Rensburg

Department of Mathematics and Statistics, York University, Toronto, Ontario, Canada M3J 1P3

E-mail: rensburg@yorku.ca

Received 2 January 2003
Published 3 April 2003
Online at stacks.iop.org/JPhysA/36/R11

Abstract

Directed square lattice models of polymers and vesicles have received considerable attention in the recent mathematical and physical sciences literature. These are idealized geometric directed lattice models introduced to study phase behaviour in polymers, and include Dyck paths, partially directed paths, directed trees and directed vesicles models. Directed models are closely related to models studied in the combinatorics literature (and are often exactly solvable). They are also simplified versions of a number of statistical mechanics models, including the self-avoiding walk, lattice animals and lattice vesicles. The exchange of approaches and ideas between statistical mechanics and combinatorics have considerably advanced the description and understanding of directed lattice models, and this will be explored in this review.

The combinatorial nature of directed lattice path models makes a study using generating function approaches most natural. In contrast, the statistical mechanics approach would introduce partition functions and free energies, and then investigate these using the general framework of critical phenomena. Generating function and statistical mechanics approaches are closely related. For example, questions regarding the limiting free energy may be approached by considering the radius of convergence of a generating function, and the scaling properties of thermodynamic quantities are related to the asymptotic properties of the generating function.

In this review the methods for obtaining generating functions and determining free energies in directed lattice path models of linear polymers is presented. These methods include decomposition methods leading to functional recursions, as well as the Temperley method (that is implemented by creating a combinatorial object, one slice at a time). A constant term formulation of the generating function will also be reviewed.

The thermodynamic features and critical behaviour in models of directed paths may be informative about the underlying properties that determine phase diagrams for wider classes of models, including physical models of polymers. Of particular interest are adsorption and collapse transitions in models of

polymers and copolymers. The properties of thermodynamic quantities in those models are described by tricritical scaling. This is reviewed for directed path models, and the generating function approaches can be used to apply tricritical scaling to models of adsorbing, inflating and collapsing directed lattice paths. Critical exponents for a variety of models can be obtained in this manner, and with it a better understanding, and a classification, of the models.

PACS numbers: 05.50.+q, 02.10.Ab, 05.40.Fb, 82.35.−x

1. Introduction

Directed lattice models of linear and branch polymers have been introduced as exactly solvable models that exhibit critical phase behaviour which is descriptive of thermodynamic behaviour seen in polymers. This phase behaviour is usually defined by considering metric and thermodynamic quantities of physical systems. Physical descriptions of the critical behaviour also include assumptions of universality; that certain scaling laws and relations are obeyed by a variety of physical and model systems, and that (in particular) the same set of critical exponents will determine transitions in a variety of different models [14, 16, 23, 24]. Most notably, model systems that idealizes a physical system may exhibit the same set of critical exponents as the physical system, and so belong to the same class. This would provide insight into the properties that determine phase behaviour.

The most important feature in models of polymers are the conformational degrees of freedom. These degrees of freedom makes a large (and sometimes dominant) contribution to the free energy via entropic terms. Thermodynamic properties of the model will generally be dependent on the relationship between conformational entropy and forces involving the polymer. Lattice models of polymers (paths in the lattice) effectively models the entropic part of the free energy, and by introducing interactions involving the path, an interacting model of a polymer is defined that may describe the phase behaviour encountered in real physical systems.

In this review the concern will be primarily on the combinatorial properties of directed square lattice path models of polymers. Such directed paths are models of linear polymers and are usually described by differential equations or by functional recursions that involve the generating function. Techniques for solving such relations will be reviewed for a directed path model of a linear polymer. Dyck paths are models of adsorbing linear polymers, and although this is one of the simplest directed path models, it still exhibits a rich phase diagram that appears to describe some of the thermodynamic properties of polymers.

Generally, the phase diagram of an interacting polymer would include a tricritical point, and the theory of tricritical scaling provides a framework for the description of the thermodynamics of directed lattice models of interacting polymers. Of particular interest in the recent literature are the phenomena of polymer adsorption and polymer collapse [14, 15, 19, 59]. These phenomena are driven by an interaction in combination with the conformational entropy of the polymer, and phase behaviour can be observed in the (statistical) geometric properties of the polymer, such as its mean size [59]. In practice, the effects of phase behaviour have also been noted in the physical behaviour of paints, coatings, adsorption of biologically important polymers and so on, and in these circumstances may be of considerable economic importance. Polymer collapse and adsorption have received attention from chemists (see for

example [32, 59]), and lattice models are motivated to give some generic insights into the theoretical issues encountered in the description of collapse and adsorption.

The most basic directed model of a polymer is a (directed) lattice path: The path starts at the origin and it steps north or east for n steps before terminating in a final vertex. It is composed of edges (steps) and vertices (sites), and is a very simple model of a linear polymer with bonds (steps) between monomers (vertices). The conformational entropy of the polymer is modeled by the large number of conformations that path may assume. These models have received considerable attention in physics [8, 9, 34, 55] and mathematics literature [27, 60].

A model of lattice paths with thermodynamic content can be created by the introduction of an *energy* in the model. For example, the energy of a lattice path of length n can be defined as the number of times a certain arrangements of edges (steps or bonds) occur in the path. Examples may include paths with energy defined as the number of vertical edges, or the number of right turns in the path. A good introduction and review of statistical mechanics and thermodynamics in lattice models of polymers is the book by Vanderzande [62].

The most important quantity in directed path models of polymers is $h_n(m)$; the number of paths of length n steps from the origin with energy equal to m. Determining $h_n(m)$ is a purely combinatorial problem, and at this level there is little (if any) physics in the analysis of these types of problems.

Statistical mechanics enters the model by the definition of a *partition function* that ultimately give rise to thermodynamic functions such as the *energy density* and the *specific heat*. These quantities usually obey certain scaling laws close to critical points, exhibit through scaling exponents whose universal character connects the combinatorial models to physical phenomena. The partition function is defined by

$$Z_n(z) = \sum_m h_n(m) z^m \tag{1}$$

where z is a *generating variable* and is said to be *conjugate* to the energy m; it is also called an *activity*, and if $z = \mathrm{e}^{\beta}$, then β is a *fugacity* (sometimes treated as proportional to the inverse of the temperature T: $\beta \propto 1/T$).

The thermodynamic nature of the lattice path can be determined by first defining a *free energy* F_n: The standard definition is

$$F_n(z) = \log Z_n(z) \tag{2}$$

and the first derivative of $F_n(z)$ to $\log z$ is the total *energy* while the second derivative to $\log z$ is the *heat capacity*. Critical behaviour is signalled by a non-analyticity in these quantities; however, since $Z_n(z)$ is a polynomial, $F_n(z)$ is analytic for $z > 0$ and so there cannot be critical phase behaviour in a model of finite size.

Phase behaviour becomes interesting in the limiting model, as the length of the path approaches infinity. In physical models this is approximated by large polymers, so that the infinite length path serves as a model for large linear polymers. Since $F_n(z)$ approaches infinity with n, a *limiting free energy density* is defined by

$$\mathcal{F}(z) = \lim_{n\to\infty} \frac{1}{n} \log Z_n(z). \tag{3}$$

Existence of this limit is not guaranteed, but is nevertheless essential for well defined models. In the models discussed in this review, it can be shown to exist in every case. It can also be shown that $\mathcal{F}(z)$ is a convex function of $\log z$ (see section 3).

Since the limiting free energy is a density (per unit length), the first derivative of $\mathcal{F}(z)$ to $\log z$ is called the *energy density* while the second derivative to $\log z$ is the *specific heat*:

$$\mathcal{E}(z) = \frac{\mathrm{d}\mathcal{F}(z)}{\mathrm{d}\log z} \qquad \mathcal{C}(z) = \frac{\mathrm{d}^2\mathcal{F}(z)}{\mathrm{d}(\log z)^2}. \tag{4}$$

The convexity properties of $\mathcal{F}(z)$ guarantees the existence of these limits for almost every z, as $n \to \infty$; these are (Lebesgue) measurable functions and $\mathcal{E}(z)$ is a non-decreasing function that is differentiable almost everywhere.

Phase transitions are classified by the continuity properties of $\mathcal{E}(z)$. A *first-order transition* occurs when there is a (jump) discontinuity in $\mathcal{E}(z)$ at a critical activity $z = z_c$. If $\mathcal{E}(z)$ is continuous, but $\mathcal{F}(z)$ is non-analytic at $z = z_c$, then the model has a *continuous transition*. In most models of this kind a continuous transition is signalled by a cusp or by a divergence at $z = z_c$ in the specific heat $\mathcal{C}(z)$. The shape of the divergence is determined by a *scaling exponent* α called the *specific heat exponent*. Traditionally (and imprecisely) this is expressed via the ansatz that

$$\mathcal{C}(z) \sim (z - z_c)^{-\alpha} \qquad \text{as } z \to z_c^+. \tag{5}$$

The precise meaning of '$\sim$' in the above is somewhat unclear, but it is usually taken to mean that $\mathcal{C}(z)$ is to leading order proportional to $(z - z_c)^{-\alpha}$. In the event that $z \to z_c^-$, then the scaling assumption may be $\mathcal{C}(z) \sim (z_c - z)^{-\alpha'}$, where α' could be numerically different from α; in some cases α' may not be defined.

The assumption in equation (5) implies that the limiting free energy should be scaling with z as

$$\mathcal{F}(z) \sim (z - z_c)^{2-\alpha} \qquad \text{as } z \to z_c^+. \tag{6}$$

It could be the case that α assumes the same value for a number of different models; in that case the models may potentially belong to the same *universality class*: these classes would share the same set of critical exponents.

The thermodynamic nature of the model is explicitly connected to the combinatorial properties by the generating function

$$G(t, z) = \sum_{n \geqslant 0} Z_n(z) t^n = \sum_{n \geqslant 0} \sum_{m \geqslant 0} h_n(m) z^m t^n \tag{7}$$

where t is the activity (generating variable) conjugate to the length of the path[1]. The radius of convergence or *critical curve* $t_c(z)$ of $G(t, z)$ is related to the limiting free energy per unit length by

$$\mathcal{F}(z) = -\log t_c(z) \tag{8}$$

and this may be observed from equation (7). One may also interpret $\log G(t, z)$ as the *grand potential* of the model. It is more often than not convenient to examine $G(t, z)$ and $t_c(z)$ directly, rather than $\mathcal{F}(z)$, in order to determine the phase behaviour and thermodynamic properties of the model [10]. More comments can be found in references [11, 35].

2. Directed paths in the square lattice

Directed lattice paths are often used as discrete models of polymers [13, 62]. These paths are often considered in the vicinity of a solid line in a model of polymer adsorption [6, 25, 44, 55, 56] and this model will be considered in section 2.2. In section 2.1 a simple model of a directed path that exhibits phase behaviour is introduced.

Let the number of directed square lattice paths with length (number of steps) n be a_n. Then $a_n = 2^n$, since each step is either in the E or the N directions. If t generates steps

[1] The generating variable t will be conjugate to path length. If $t \to \sqrt{s}$, then s will be conjugate to the half-length of the path. The activity q will be conjugate to areas enclosed by paths, and z will be an activity that is generically conjugate to an energy.

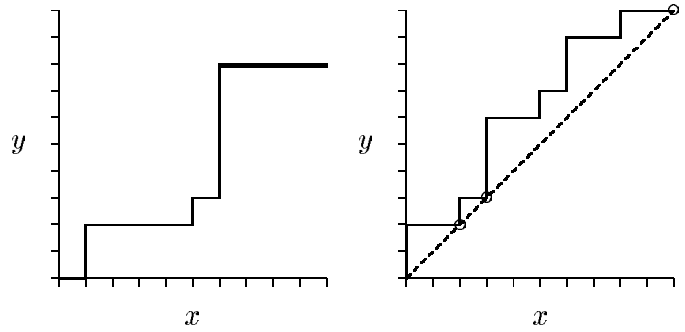

Figure 1. Two models of directed paths. On the left is a directed path consisting of *choice edges* followed by a sequence of edges fixed horizontally. Choice edges are weighted by a factor of z each. On the right is a Dyck path interacting with the main diagonal. Visits of the path to the main diagonal are denoted by $\circ$, and each are weighted by a factor of z in the generating function.

(and thus the length of the paths), then the generating function is $(1-2t)^{-1}$; it has radius of convergence $t_c = 1/2$ and a simple pole singularity at this point.

This model can be changed into a simple lattice model of a polymer with a bending energy. Let $a_n(m)$ be the number of directed paths with n steps and exactly m right angles between successive steps (that is, vertices where an N steps follows an E step, or vice versa). Then $a_n(m) = 2\binom{n-1}{m}$ if $n \geqslant 1$ (but note that $a_0(0) = 1$), and the extra factor of 2 accounts for the two possible choices for the first step in the walk. If s is the activity conjugate to the energy (the number of right angles), then the full generating function is

$$g_0(t,z) = 1 + \sum_{n\geqslant 1}\left[\sum_{m=0}^{n-1} a_n(m) z^m\right] t^n = 1 + \frac{2}{(1+z)(1-t(1+z))}. \tag{9}$$

There is a simple pole in this model at $t_c(z) = 1/(1+z)$, so that the limiting free energy can be determined immediately:

$$\mathcal{F}(z) = \log(1+z). \tag{10}$$

This free energy is analytic for all $z > 0$, so that there is no critical behaviour, and it is not interesting from a thermodynamic point of view. It is not difficult to construct models of directed paths with interesting phase behaviour.

2.1. A directed path with fixed edges

Consider a directed path of length n with the property that the first m edges could be oriented either E or N (and are called *choice edges*), and the remaining $n-m$ edges are all constrained to point E (see figure 1) [35]. The number of such paths is $a_n(m) = 2^m$, and the generating function is

$$g(t,z) = \frac{1}{(1-t)(1-2tz)}. \tag{11}$$

The critical curve $t_c(z)$ is directly seen from $g(t,z)$ to be given by

$$t_c(z) = \begin{cases} 1 & \text{if} \quad z \leqslant \frac{1}{2} \\ \frac{1}{2z} & \text{if} \quad z > \frac{1}{2} \end{cases} \tag{12}$$

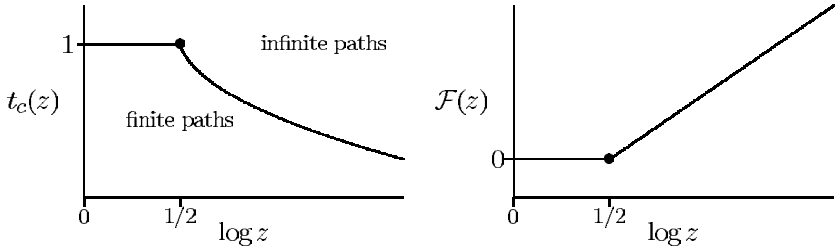

Figure 2. Graphs of the critical curve $t_c(z)$ of the generating function $g(t, z)$ for a directed path with choice edges, and the limiting free energy $\mathcal{F}(z)$ of this model, as discussed in section 2.1. The critical point $z_c = 1/2$ is found at a non-analyticity in $\mathcal{F}(z)$. The discontinuity in the first derivative of $\mathcal{F}(z)$ to $\log z$ indicates that this is a first-order phase transition. If $z > z_c$, then the density of choice edges is equal to one (as seen from equation (14)), while this density is zero if $z < z_c$.

The limiting free energy is obtained by calculating $\log t_c(z)$, and is given by (see figure 2)

$$\mathcal{F}(z) = \begin{cases} 0 & \text{if} \quad z \leqslant \frac{1}{2} \\ \log 2 + \log z & \text{if} \quad z > \frac{1}{2}. \end{cases} \tag{13}$$

The first derivative of the limiting free energy to $\log z$ is the energy density, and this is given by

$$\mathcal{E}(z) = \begin{cases} 0 & \text{if} \quad z < \frac{1}{2} \\ 1 & \text{if} \quad z > \frac{1}{2} \end{cases} \tag{14}$$

so that this model has a first-order transition at $z_c = 1/2$. It is possible to determine the critical exponent α in equation (6). Observe that if $z > 1/2$, then one may expand $\mathcal{F}(z)$:

$$\begin{aligned} \mathcal{F}(z) &= \log\left(1 + \left(z - \tfrac{1}{2}\right)\big/\tfrac{1}{2}\right) \\ &= 2\left(z - \tfrac{1}{2}\right) + \left(2\left(z - \tfrac{1}{2}\right)\right)^2 + O\left(\left(2\left(z - \tfrac{1}{2}\right)\right)^3\right). \end{aligned} \tag{15}$$

Comparison with equation (6) shows that $2 - \alpha = 1$, or that $\alpha = 1$, by considering the leading order term in $\mathcal{F}(z)$; this value if consistent with a first-order transition in this model. If $t < t_c(z)$, then the generating function in this model is finite, and its value is determined by contributions by paths of *finite length*. Hence, the *phase* determined by $t < t_c(z)$ is the *finite* phase in this model. Conversely, if $t > t_c(z)$, then $g(t, z)$ is infinite due to the contributions of paths of arbitrary length[2]; this phase is the *infinite* phase, as marked in figure 2. These two phases are separated by the *critical curve* $t = t_c(z)$, and at the critical point $z = z_c = 1/2$ there is a non-analyticity in $t_c(z)$ that corresponds to the first-order phase transition as observed from the limiting free energy in equation (13).

The entire critical curve $t_c(z)$ in this model is the locus of simple poles in $g(t, z)$, except when $z = z_c = 1/2$, where a second-order pole is encountered. The shape of the critical curve is determined by equation (12), and by expanding the critical point, $1 - t_c(z) = 2(z - 1/2) + O((z - 1/2)^2)$, so that $1 - t_c(z)$ increases linearly with z. This is the *shape* of the critical curve, and it will play a role in describing the critical properties of the model.

[2] It is in principle still possible to fix t and z in this regime and then consider a model of the path confined to a finite maximum volume (or of finite maximum length). Taking the maximum to infinity with appropriate normalization may then define a thermodynamic limit. The existence of this limit is a separate question that will not be discussed in this review.

2.2. Dyck paths adsorbing in the main diagonal

A *Dyck path* is a directed path from the origin in the square lattice, constrained so that its first and last vertices are in the main diagonal. Otherwise it steps only on vertices in the half-space $y \geqslant x$ above or on the main diagonal [26, 27, 34, 60]. An example of a Dyck path is illustrated in figure 1.

A two-dimensional directed model of polymer adsorption can be constructed by adding an interaction between a Dyck path and the main diagonal [34], see also [6, 13, 25, 35, 55]. The generating function of this model can be found by determining and then solving a functional recursion that the generating function must satisfy.

An *excursion* is a Dyck path that has no vertices, except its terminal (first and last) vertices, in the main diagonal. It is the case that Dyck paths of length $2n$ are in one-to-one correspondence with excursions of length $2n + 2$. To see this, note that a Dyck path can be turned into an excursion by translating it one step in the y-direction, and then adding two new edges to reconnect the endpoints to the main diagonal. This construction is uniquely reversible, and it establishes a bijection between Dyck paths and excursions.

The number of Dyck paths of length n steps is denoted by C_n. An explicit expression for C_n can be obtained as follows: Consider a staircase walk ω from the origin $(0, 0)$ to the point (n, n), and suppose that it has l left turns. The x-coordinates of these left turns can be chosen in $\binom{n}{l}$ ways, and the y-coordinates can similarly be chosen in $\binom{n}{l}$ ways. Thus, the coordinates of the l left turns can be chosen in $\binom{n}{l}^2$ ways altogether.

On the other hand, ω would not be a Dyck path if it visits vertices below the main diagonal. Hence, paths that visit vertices below the main diagonal must be subtracted from $\binom{n}{l}^2$ so that only Dyck paths remain. Suppose that ν is a directed path and that it visits a *last* vertex v in the subdiagonal $y = x - 1$. A reflection of that segment of ν from v to (n, n) through the subdiagonal gives a directed path ending in the vertex with coordinate $(n + 1, n - 1)$. On the other hand, a directed path ν' that ends in $(n + 1, n - 1)$ must visit a last vertex v' in the subdiagonal, and so the segment from v' to $(n + 1, n - 1)$ can be reflected to give a staircase path ending in (n, n) that visits at least one vertex below the diagonal. This establishes a one-to-one correspondence between staircase paths from the origin to $(n+1, n-1)$, and Dyck paths from the origin to (n, n) that visits at least one vertex below the main diagonal.

The number of staircase walks ending in $(n + 1, n - 1)$ with l left turns is $\binom{n+1}{l}\binom{n-1}{l}$; to see this one uses an argument similar to the previous by selecting first an x-coordinate, and then a y-coordinate, for all the left turns in the path. Thus, the number of Dyck paths of length $2n$ (or of half-length n) is given by

$$C_n = \sum_{l=0}^{n} \binom{n}{l}\binom{n}{l} - \sum_{l=0}^{n-1} \binom{n+1}{l}\binom{n-1}{l} = \frac{1}{n+1}\binom{2n}{n}. \tag{16}$$

C_n is also known as *Catalan's number*; there are many sequences of objects known to be enumerated by C_n, for example, there are connections to the gambler's ruin problem [21].

The generating function of Dyck paths, with t conjugate to length, can now be determined:

$$C(t) = \sum_{n=0}^{\infty} C_n t^{2n}. \tag{17}$$

An explicit closed form expression for $C(t)$ can be obtained by using excursions and by classifying Dyck paths as either being a single vertex at the origin (the trivial path), or as consisting of an excursion followed by a Dyck path that may be trivial.

Excursions of length $2n + 2$ are in one-to-one correspondence with Dyck paths of length $2n$, so it follows that excursions are generated by $t^2C(t)$. Any Dyck path is either a single

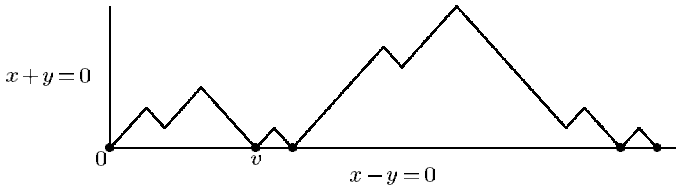

Figure 3. A Dyck path in the square lattice. The horizontal axis is the main diagonal, and the vertical axis the anti-diagonal. Vertices in the main diagonal, marked by •, are *visits*. A Dyck path with no visits, except its first and last vertices, is an *excursion*. Dyck paths are in one-to-one correspondence with excursions: to see this, note that every Dyck path can be turned into an excursion by adding one edge at each of its endpoints, and then translating it one step away from the main diagonal. This is uniquely reversible. Dyck paths may be decomposed into an excursion, followed by an arbitrary Dyck path (that may be a single visit) by cutting it into two parts on its first return v to the main diagonal.

vertex, or starts with an excursion and after its first return to the main diagonal may either terminate, or continue as an arbitrary Dyck path. Thus

$$C(t) = 1 + [t^2 C(t)]C(t). \tag{18}$$

Solving for $C(t)$ from equation (18) shows that

$$C(t) = \frac{2}{1+\sqrt{1-4t^2}} = \frac{1-\sqrt{1-4t^2}}{2t^2} \tag{19}$$

and note that $C(t)$ has radius of convergence $t_c = 1/2$ given by the square root branch point.

A Dyck path is *adsorbing* if its visits to the main diagonal are generated by an activity z. Let the generating function of adsorbing Dyck paths be $C(t, z)$, and note that each adsorbing Dyck path is either a single visit at the origin, or is composed of an excursion up to its first return to the main diagonal (see figure 3), followed by an arbitrary adsorbing Dyck path. In other words

$$C(t, z) = z + z[t^2 C(t)]C(t, z) \tag{20}$$

where $C(t) \equiv C(t, 1)$ and is given by equation (19). If $z = 1$ in this recurrence, then $C(t, 1)$ can be found. Subsequently, one may solve for $C(t, z)$,

$$C(t, z) = \frac{2z}{2 - z(1-\sqrt{1-4t^2})}. \tag{21}$$

The generating function $C(t, z)$ satisfies an *exchange relation* [57]:

$$zC(t, z)(C(t, 1) - 1) = C(t, 1)(C(t, z) - z) \tag{22}$$

that is invariant under the exchange $1 \leftrightarrow z$. This can be checked by direct substitution of $C(t, z)$, but more insight is gained by proving it explicitly.

Consider a non-trivial Dyck path, and suppose that the visits to the main diagonal are weighted from the origin by z, but that this process is incomplete—there is a last weighted visit v, and every visit preceding v is weighted by z, while every visit after v is weighted by 1. Suppose also that v is not the final vertex in the path. Such partially weighted paths are generated by $C(t, z)\,(C(t, 1) - 1)$, since the weighted part of the path is generated by $C(t, z)$, and may consist of a single vertex. The part of the path following v may not be a trivial path (since v is not the final vertex in the path), and so it is generated by $(C(t, 1) - 1)$.

Consider now, instead, the case that the first visit w following v is provided with a factor of z. w may be the final vertex in the path, and the weighed part of the path contains at least

the two visits v and w. The resulting path consists of a first weighted part ending in w (and it may not be trivial) generated by $(C(t,z)-z)$, followed by an unweighted path following w (that may be trivial) and is generated by $C(t,1)$. Since the only additional factor was z appended to w, this shows that $C(t,z)\,(C(t,1)-1)$ and $C(t,1)\,(C(t,z)-z)$ differs only by one factor of z. This proves equation (22). One may solve for $C(t,z)$ from equation (22) to obtain

$$C(t,z)=\frac{zC(t,1)}{z+(1-z)C(t,1)}. \tag{23}$$

A solution for $C(t,1)$ cannot be obtained from this relation, and so it is not possible to solve for $C(t,z)$. In other words, this relation is essentially different from equation (20). It will be useful in finding generating functions for a model of adsorbing and coloured Dyck paths in section 2.6.3.

The critical curve $t_c(z)$ of $C(t,z)$ may be computed from equation (21). Direct computation gives

$$t_c(z)=\begin{cases}\frac{1}{2} & \text{if} \quad z\leqslant 2\\ \frac{\sqrt{z-1}}{z} & \text{if} \quad z>2\end{cases} \tag{24}$$

and so the limiting free energy in this model is

$$\mathcal{F}(z)=\begin{cases}\log 2 & \text{if} \quad z\leqslant 2\\ \log z-\frac{1}{2}\log(z-1) & \text{if} \quad z>2.\end{cases} \tag{25}$$

In other words, the adsorption transition is at $z_c=2$. Note that the energy is given by

$$\mathcal{E}(z)=\begin{cases}0 & \text{if} \quad z\leqslant 2\\ \frac{z-2}{2z-2} & \text{if} \quad z>2.\end{cases} \tag{26}$$

There is a cusp singularity in the specific heat

$$\mathcal{C}(z)=\begin{cases}0 & \text{if} \quad z\leqslant 2\\ \frac{z}{2(z-1)^2} & \text{if} \quad z>2.\end{cases} \tag{27}$$

A schematic plot of $t_c(z)$ and $\mathcal{F}(z)$ against $\log z$ will again appear as in figure 2, although now $\mathcal{F}(z)$ is not linear in $\log z$ for $z>z_c$. Expanding $\mathcal{F}(z)$ about $z_c=2$,

$$\mathcal{F}(z)=\log 2+\tfrac{1}{8}(z-2)^2-\tfrac{1}{8}(z-2)^3+O((z-2)^4) \qquad \text{for} \quad z\to z_c^+ \tag{28}$$

and comparing it with equation (6) shows that the specific heat exponent is $2-\alpha=2$, or that $\alpha=0$. The energy $\mathcal{E}(z)$ is continuous at $z=z_c$, so this model has a continuous transition, as opposed to the first-order transition in the model with choice edges. Note that $\mathcal{E}(z)$ increases from zero continuously with increasing z, and that asymptotically every second vertex in the path becomes a visit, as one sees from equation (26).

2.3. A directed path adsorbing in the main diagonal (or a defect plane)

The generating function $C(t)$ for Dyck paths can be used to determine the generating function of directed paths interacting with a (penetrable) main diagonal (called a *defect plane*). In figure 4 a directed path starts at the origin, and returns to the main diagonal a first time at v, and a last time at w, before it wanders off in the lattice in the space either above the defect plane.

The last segment of the path, following the last visit w, is its *tail*, and it may be empty if the last vertex in the path is also its last visit w. Suppose that $D(t,z)$ is the generating function

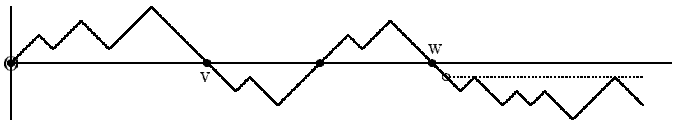

Figure 4. A directed path from the origin with the main diagonal oriented horizontally. This path returns to the main diagonal first time at v, and a last time at w. It then continues as a directed path in the space under the main diagonal in the first quadrant of the square lattice.

of directed paths with empty tails. A directed path counted by $D(t, z)$ may consist of a single vertex, or may contain at least two edges. If such a path contains at least two edges, then it may be cut at the first return v to the main diagonal to find an excursion, or an excursion reflected in the main diagonal, and a remaining arbitrary directed path without a tail (that may be the trivial path). Therefore,

$$D(t, z) = z + z[t^2C(t) + t^2C(t)]D(t, z) \tag{29}$$

where the first term accounts for directed paths composed of a single vertex at the origin, and $t^2C(t)$ is the generating function of excursions. Solving for $D(t, z)$ shows that

$$D(t, z) = \frac{z}{1 - 2zt^2C(t)} = \frac{z}{1 - z(1 - \sqrt{1 - 4t^2})} = \frac{1}{2}C(t, 2z) \tag{30}$$

by comparison with equation (21).

The full generating function of adsorbing directed paths, which includes tails, can be found by first considering Dyck paths with tails. This will enable us to find a generating function for tails, and that can be appended to equation (30). Suppose that Dyck paths with tails are generated by $C_t(t)$. By noting that each such path is either a Dyck path (without a tail) or a Dyck path with a tail of at least one edge (generated by $C(t)tC_t(t)$) (since $tC_t(t)$ generates directed paths which start from the origin and never returns to the main diagonal), it follows that

$$C_t(t) = C(t) + [tC(t)]C_t(t). \tag{31}$$

Therefore,

$$C_t(t) = \frac{C(t)}{1 - tC(t)} = \frac{1 - 2t - \sqrt{1 - 4t^2}}{2t(2t - 1)}. \tag{32}$$

A tail can be added to an adsorbing Dyck path by noting that $(1 + tC_t(t))$ generates either an empty tail, or a tail above the main diagonal. Thus, $C_t(t, z) = C(t, z)(1 + tC_t(t))$ is the generating function of adsorbing Dyck paths with tails, where $C(t, z)$ is given by equation (21). Simplifying the expression shows that

$$C_t(t, z) = \frac{z(1 - 2t + \sqrt{1 - 4t^2})}{(1 - 2t)(2 - z(1 - \sqrt{1 - 4t^2}))}. \tag{33}$$

In other words, $C_t(t, z)$ has singularities whenever $t = 1/2$ or $2 - z(1 - \sqrt{1 - 4t^2}) = 0$. Hence, $C_t(t, z)$ is convergent whenever $t < \min\{1/2, \sqrt{z - 1}/z\}$, and the radius of convergence is given by

$$t_c(z) = \begin{cases} \frac{1}{2} & \text{if} \quad z \leqslant 2 \\ \frac{\sqrt{z-1}}{z} & \text{if} \quad z > 2. \end{cases} \tag{34}$$

In other words, the adsorption transition is still at $z_c = 2$, and the tail does not affect the location of the critical point.

The generating function $(1 + tC_t(t) + tC_t(t))$ may be appended to the generating function $D(t, z)$ in equation (30) to obtain the full generating function of a directed path that interacts with the main diagonal:

$$D_t(t, z) = D(t, z)[1 + 2tC_t(t)] = \frac{z\sqrt{1-4t^2}}{(1-2t)(1-z(1-\sqrt{1-4t^2}))}. \tag{35}$$

There are (again) square root singularities in $D_t(t, z)$ at $t = 1/2$. There are also simple poles along the solution of $1 - z(1 - \sqrt{1-4t^2}) = 0$. Solving for the critical values of t shows that either $t = 1/2$, or $t = \sqrt{2z-1}/2z$. Hence

$$t_c(z) = \begin{cases} \frac{1}{2} & \text{if} \quad z \leqslant 1 \\ \frac{\sqrt{2z-1}}{2z} & \text{if} \quad z > 1. \end{cases} \tag{36}$$

The critical point is at $z_c = 1$, and the limiting free energy is given by

$$\mathcal{F}(z) = \begin{cases} \log 2 & \text{if} \quad z \leqslant 1 \\ \log 2 + \log z - \frac{1}{2}\log(2z-1) & \text{if} \quad z > 1. \end{cases} \tag{37}$$

As before, expanding the limiting free energy for $z \to z_c^+$ gives

$$\mathcal{F}(z) = \log 2 + \tfrac{1}{2}(z-1)^2 - (z-1)^3 + O((z-1)^4) \tag{38}$$

so that comparison with equation (6) indicates that the specific heat exponent is $\alpha = 0$. The energy $\mathcal{E}(z)$ is given by

$$\mathcal{E}(z) = \begin{cases} 0 & \text{if} \quad z \leqslant 1 \\ \frac{z-1}{2z-1} & \text{if} \quad z > 1 \end{cases} \tag{39}$$

and the specific heat in this model is given by

$$\mathcal{C}(z) = \begin{cases} 0 & \text{if} \quad z \leqslant 1 \\ \frac{z}{(2z-1)^2} & \text{if} \quad z > 1. \end{cases} \tag{40}$$

Thus, this is again a continuous adsorption transition, as obtained for Dyck paths in section 2.2. Comparison with equations (26) and (27) shows that this model is very similar to adsorbing Dyck paths; they are asymptotically the same.

2.4. The Temperley method and adsorbing Dyck paths

The generating functions for adsorbing Dyck paths and adsorbing directed paths above were all obtained by dissecting the paths resulting in a decomposition of the generating function that gives a functional equation that may be solved. This method is powerful, and can be used effectively in a large number of different models. It is also called a 'wasp-waiste' method (since it cuts the object at a narrow part), or 'factorization' method [53].

Not all models may be treated by using a factorization method. The *Temperley method* is an alternative that may be used in some cases. This method constructs the object a slice at time, and the specifics are dependent on the particular model. For adsorbing Dyck paths, let $C_e(s; t, z)$ be the generating function of *left factors* of *even length* of adsorbing Dyck paths. The activities t and z are introduced conjugate to length and to visits respectively, and an activity s will be conjugate to the height of the last vertex above the adsorbing main diagonal.

An even left factor of a Dyck path may be extended by two steps if two more edges are added to its last vertex. This may or may not change the height of the last vertex. If two steps are appended, both away from the main diagonal (or 'up'), then a factor of $t^2 s$ should be introduced. If one step is appended 'up', and the second 'down', or vice versa, then there is no

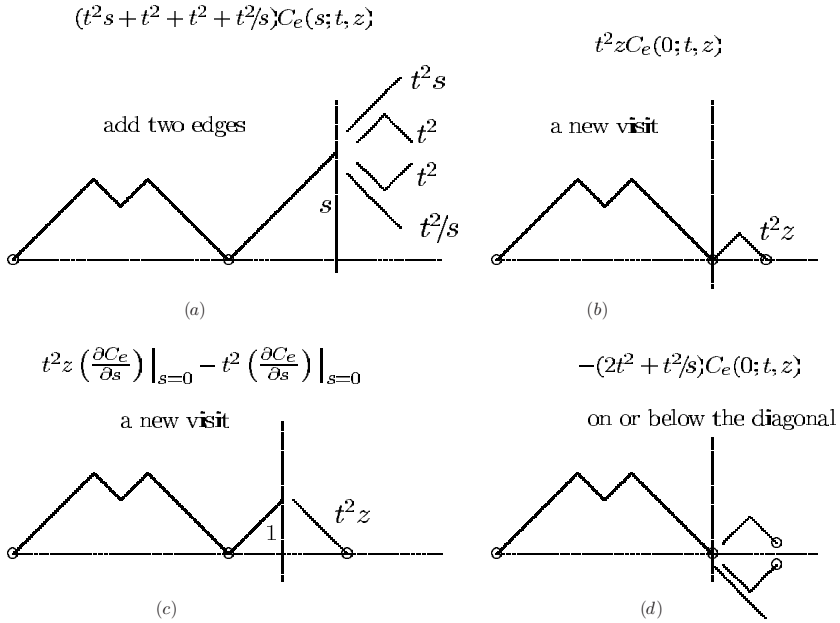

Figure 5. The generating function $C_e(s;t,z)$ of even length left factors of adsorbing Dyck paths with activity s conjugate to the height of the last vertex can be determined by using the Temperley method to add two more steps to such Dyck paths. In (a) it is noted that two more steps can be added in four ways, generating $(t^2s+t^2+t^2+t^2/s)C_e(s;t,z)$. New visits can be created as in (b) or in (c). First observe that $C_e(0;t,z)$ generates Dyck paths with last vertex in the main diagonal, so that the two steps added in (b) creates a new visit, and this would be generated by $t^2zC_e(0;t,z)$. This term is also (incorrectly) included in (a) as $t^2C_e(s;t,z)_{s=0}$, and is duly cancelled in (d), where paths that step below the main diagonal are also removed. Finally, note that $(\frac{\partial C_e}{\partial s})_{s=0}$ generates Dyck paths that terminates at height $h=1$ above the main diagonal. A new visit may be created as in (c), and the factor $t^2z(\frac{\partial C_e}{\partial s})_{s=0}$ is included while the factor $t^2(\frac{\partial C_e}{\partial s})_{s=0}$ is removed to include a weight z for the new visit. Finally, a path may consist of a single visit at the origin.

change in the height of the last vertex, and the factor (t^2+t^2) is obtained. Finally, there may be two steps 'down', this corresponds to the factor t^2/s. Thus, the factor $(t^2s+t^2+t^2+t^2/s)$ generates additional two steps to a left factor of a Dyck path. Appending this to $C_e(s;t,z)$ will lengthen the Dyck path by two steps, but this must be corrected if new visits are generated, or if the path steps below the main diagonal.

In figure 5 the construction of a mixed differential and functional equation for $C_e(s;t,z)$ is demonstrated by using the Temperley method. By following the arguments in figure 5, we obtain the result that

$$C_e(s;t,z) = z + t^2(s+2+s^{-1})C_e(s;t,z) + t^2(z-2-s^{-1})C_e(0;t,z) + t^2(z-1)\left(\frac{\partial C_e}{\partial s}\right)_{s=0}. \tag{41}$$

In order to solve this equation, first observe that the quantities $C_e(0;t,z)$ and $\left(\frac{\partial C_e}{\partial s}\right)_{s=0}$ are unknown, and once they are determined, an expression for $C_e(s;t,z)$ will be known.

By first noting that $\lim_{s\to 0^+}[C_e(s;t,z)-C_e(0;t,z)]/s = \left(\frac{\partial C_e}{\partial s}\right)_{s=0}$, and then taking $s\to 0^+$ in equation (41), one finds that

$$C_e(0;t,z) = z + zt^2C_e(0;t,z) + zt^2\left(\frac{\partial C_e}{\partial s}\right)_{s=0}. \tag{42}$$

Solving for $\left(\frac{\partial C_e}{\partial s}\right)_{s=0}$ in terms of $C_e(0; t, z)$, and substituting into equation (41), then gives

$$z(1 - t^2(s + 2 + s^{-1}))C_e(s; t, z) = z + (z - 1 - zt^2 - zt^2 s^{-1})C_e(0; t, z). \tag{43}$$

This equation can now be solved using the *kernel method* [1, 4].

Observe that $C_e(0; t, z)$ is an even left factor and that its final vertex is a visit in the main diagonal—that is, these are Dyck paths in the length-visit ensemble. The generating function of these objects were determined in section 2.2, and is explicitly given in equation (21). The kernel method will again give an expression for $C_e(0; t, z)$. The method is implemented by assuming that $C_e(0; t, z)$ is a power series in t and in z. If s is selected on the left-hand side of equation (43) to be a root of $(1 - t^2(s + 2 + s^{-1}))$, then $C_e(0; t, z)$ can be determined. The roots are

$$s_- = \frac{1 - \sqrt{1 - 4t^2}}{2t^2} - 1 \qquad \text{and} \qquad s_+ = \frac{1 + \sqrt{1 - 4t^2}}{2t^2} - 1. \tag{44}$$

Only the choice to substitute $s = s_-$ in equation (43) gives a power series solution for $C_e(0; t, z)$ with non-negative coefficients: The result is that $C_e(0; t, z) = C(t, z)$ with $C(t, z)$ given in equation (21).

Finally, one may solve directly for $C_e(s; t, z)$ by substituting $C_e(0; t, z)$ in equation (43). The result is that

$$C_e(s; t, z) = \frac{2zt^2 - sz(1 - 2t^2 + \sqrt{1 - 4t^2})}{(t^2(s + 1)^2 - s)(2 - z(1 - \sqrt{1 - 4t^2}))}. \tag{45}$$

The phase diagram of this model can be determined by solving for $t_c(s, z)$, the radius of convergence of $C_e(s; t, z)$. There are several sources for singularities in $C_e(s; t, z)$, namely a branch point due the square root radical, and simple poles when one or the other factor in the denominator vanishes. This shows that

$$t_c(s, z) = \min\left\{\frac{1}{2}, \frac{\sqrt{s}}{s + 1}, \frac{\sqrt{z - 1}}{z}\right\}. \tag{46}$$

Solving explicitly for $t_c(s, z)$ from this gives

$$t_c(s, z) = \begin{cases} \frac{1}{2} & \text{if} \quad s \geqslant 1 \quad \text{and} \quad z \leqslant 2 \\ \frac{\sqrt{s}}{s+1} & \text{if} \quad s \leqslant \min\left\{1, \frac{1}{z-1}\right\} \\ \frac{\sqrt{z-1}}{z} & \text{if} \quad s \geqslant \frac{1}{z-1} \quad \text{and} \quad z \geqslant 2. \end{cases} \tag{47}$$

This result identifies three thermodynamic phases in this model, and the phase diagram in the sz-plane is plotted in figure 6. If $s < \min\{1, 1/|z - 1|\}$ for any z then a desorbed phase of paths with endpoint 'close' to the adsorbing line is obtained. In the scaling limit this model would be indistinguishable from a model of desorbed Dyck paths. If $s > 1$ and $z < 2$ then conformations of paths that are desorbed and that have endpoints detached from the adsorbing line are favoured. This is a phase of desorbed paths with unattached endpoints. Finally, a phase with $z > 2$ and $s > 1/(z - 1)$ favours adsorbed paths (with a non-negative density of visits). The density of visits favours conformations with endpoints close to the adsorbing line, and this phase will be indistinguishable from a phase of adsorbed Dyck paths.

This model is a three-parameter model, and the phase diagram in figure 6 is the projection of a critical surface $t_c(s, z)$ that separates a phase of finite length paths (if $t < t_c(s, z)$) from a phase of infinite length paths (if $t > t_c(s, z)$). The transition from finite length paths to infinite length paths goes through one the three critical surfaces identified in figure 6. The meeting point of the three phases at $(z, s) = (2, 1)$ is a *triple point*.

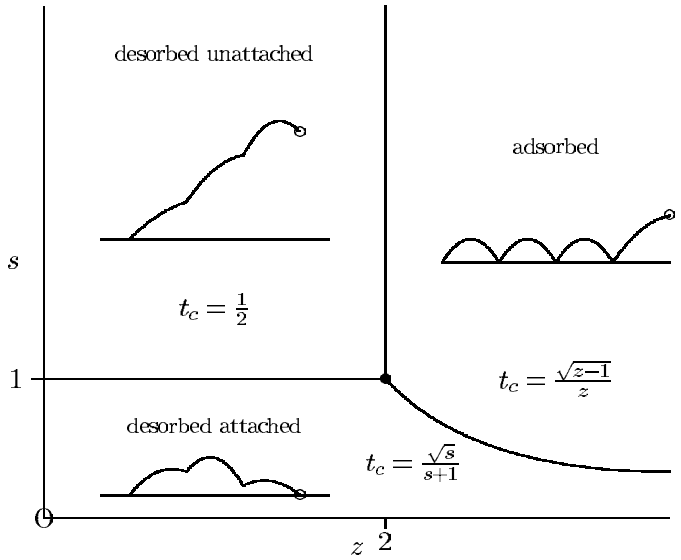

Figure 6. The phase diagram of adsorbing Dyck paths with a tail and endpoint weighted by s. There are three phases in this diagram: (1) a desorbed phase with an attached endpoint if s and z are both small, (2) a desorbed phase with a free endpoint if s is large and z is small, and (3) an adsorbed phase. These three phases meet along three critical curves that marks the transitions between the singularities that determine the radius of convergence of $C_e(s; t, z)$. The phases also meet at a triple point located at $s = 1$ and $z = 2$ in the phase diagram. This shows that the adsorption transition in the two-parameter model (which is equivalent to putting $s = 1$ in this model) in section 2.2 is a multicritical point.

The complete generating function of this model can be obtained by first determining $C_o(s; t, z)$, the generating function of odd length paths. This is readily found by adding a single step to the paths counted by $C_e(s; t, z)$, giving the relation

$$C_o(s; t, z) = t(s + s^{-1})C_e(s; t, z) - ts^{-1}C_e(0; t, z) \tag{48}$$

where the last term subtracts paths with a step below the main diagonal, and note that no new visits can be created by adding a single step. Adding these paths to $C_e(s; t, z)$ gives the full generating function that may be simplified to

$$C(s; t, z) = \frac{z(2t(1-t)(1+2t) - (s+ts^2+t)(1-2t^2+\sqrt{1-4t^2}))}{(t^2(s+1)^2 - s)(2 - z(1-\sqrt{1-4t^2}))}. \tag{49}$$

Putting $s = 1$ in this expression to recover

$$C(1; t, z) = \frac{z(1-2t+\sqrt{1-4t^2})}{(1-2t)(2 - z(1+\sqrt{1-4t^2}))} \tag{50}$$

the generating function of adsorbing Dyck paths with a tail, as also obtained in equation (33). Finally, putting $z = 1$ should give the generating function of Dyck paths with a tail

$$C_t(t) = C(1; t, 1) = \frac{1-2t-\sqrt{1-4t^2}}{2t(2t-1)} \tag{51}$$

as found in equation (32).

If $z = 1$ in equation (49), then a model of Dyck paths with a tail and a weighted endpoint is found. The generating function for this model is

$$C(s; t, 1) = \frac{2t(1-t)(1+2t) - (s+ts^2+t)(1-2t^2+\sqrt{1-4t^2})}{(t^2(s+1)^2 - s)(1+\sqrt{1-4t^2}))}. \tag{52}$$

The critical curve is given by

$$t_c(s) = \begin{cases} \frac{1}{2} & \text{if} \quad s \leqslant 1 \\ \frac{\sqrt{s}}{s+1} & \text{if} \quad s > 1. \end{cases} \tag{53}$$

The free energy for this model is

$$\mathcal{F}_s(s) = \begin{cases} \log 2 & \text{if} \quad s \leqslant 1 \\ \log(s+1) - \frac{1}{2}\log s & \text{if} \quad s > 1 \end{cases} \tag{54}$$

On the other hand, for paths critical with respect to adsorption, $z = 2$, and the generating function becomes

$$C(s; t, 2) = \frac{2t(1-t)(1+2t) - (s + ts^2 + t)(1 - 2t^2 + \sqrt{1-4t^2})}{(t^2(s+1)^2 - s)\sqrt{1-4t^2}}. \tag{55}$$

The critical curve in this case is also given by equation (53). Note that $C(s; t, 1)$ is finite along the critical curve $t_c(s)$ for $s < 1$, but that $C(s; t, 2)$ is infinite here.

2.5. The constant term formulation of adsorbing Dyck paths

The adsorbing Dyck path may be formulated as a difference equation problem with a boundary condition that accounts for the interaction between the path and the adsorbing diagonal. This difference equation may be solved by a *constant term formula* [6]. This technique is technically much more difficult to use than generating function approaches derived from a Temperley or decomposition method, but it has the advantage that expressions for the partition function of the problem can also be found.

The appropriate differential equation for adsorbing Dyck paths may be found by first noting that there is a bijection from Dyck paths onto random walks from the origin on the non-negative integer axis. This map is most easily described by projecting the Dyck path into the anti-diagonal in the square lattice to obtain a random walk that starts and terminates at the origin, and otherwise steps only on that half of the anti-diagonal with non-negative y-coordinates.

Let $v_n(j; j_0)$ be the number of random walks from $j_0 \geqslant 0$; on the non-negative integer line, ending in the vertex j, and with each random walk weighted by z^v where v is the number of visits of the random walk to the origin at $j = 0$. Then $v_n(j; j_0)$ is the partition function of directed paths of length n, starting at height j_0, and ending at height j, above the main diagonal, and with visits to the main diagonal weighted by z. Continue by suppressing the explicit dependence on j_0, and note that $v_n(j) \equiv v_n(j; j_0)$ satisfies the difference equation

$$\begin{aligned} &v_n(j) = v_{n-1}(j-1) + v_{n-1}(j+1) \qquad \forall j \geqslant 1 \quad \text{and} \quad \forall n \geqslant 1 \\ &v_n(0) = z v_{n-1}(1) \qquad \forall n \geqslant 1 \end{aligned} \tag{56}$$

where the boundary condition picks up factors of z each time the random walk visits the origin. The function

$$q_n(j) = (\mathrm{e}^{\mathrm{i}k} + \mathrm{e}^{-\mathrm{i}k})^n (A_1 \mathrm{e}^{\mathrm{i}jk} + A_2 \mathrm{e}^{-\mathrm{i}jk}) \tag{57}$$

is a solution of equation (56) for any real choice of $k \in (-\pi, \pi]$, due to the periodicity of the complex exponentials. Substitution of (57) into (56) shows that

$$\frac{A_1}{A_2} = -\frac{(\mathrm{e}^{\mathrm{i}k} + \mathrm{e}^{-\mathrm{i}k}) - z\,\mathrm{e}^{-\mathrm{i}k}}{(\mathrm{e}^{\mathrm{i}k} + \mathrm{e}^{-\mathrm{i}k}) - z\,\mathrm{e}^{\mathrm{i}k}} = \mathcal{S}(k). \tag{58}$$

The *scattering function* $\mathcal{S}(k)$ describes the scattering of the walk from the origin via the boundary condition in equation (56). The full solution of equation (56) is

$$v_n(j) = \int_{-\pi}^{\pi} A_2(\mathrm{e}^{\mathrm{i}k} + \mathrm{e}^{-\mathrm{i}k})^n [\mathrm{e}^{-\mathrm{i}jk} + \mathcal{S}(k)\,\mathrm{e}^{\mathrm{i}jk}]\,\mathrm{d}k. \tag{59}$$

In this expression A_2 is an arbitrary function of k, and it should be fixed by the initial condition of the walk: the walk started at j_0. It also follows from equation (57) that reversal of the walk occurs if $k \to -k$. The factor $(\mathrm{e}^{\mathrm{i}k} + \mathrm{e}^{-\mathrm{i}k})^n$ in equation (59) generates n steps in the walk, and so one should take $n = 0$, $j = j_0$ and $k \to -k$ to fix the initial position of the walk at $j = j_0$. Thus,

$$A_2 = C_0[\mathrm{e}^{\mathrm{i}j_0k} + \mathcal{S}(-k)\,\mathrm{e}^{-\mathrm{i}j_0k}] \tag{60}$$

in equation (59), and note that $\mathcal{S}(-k) = 1/\mathcal{S}(k)$ to obtain an integral expression for $v_n(j) \equiv v_n(j; j_0)$:

$$v_n(j) = C_0 \int_{-\pi}^{\pi} (\mathrm{e}^{\mathrm{i}k} + \mathrm{e}^{-\mathrm{i}k})^n [\mathrm{e}^{\mathrm{i}(j-j_0)k} + \mathcal{S}(k)\,\mathrm{e}^{\mathrm{i}(j+j_0)k}]\,\mathrm{d}k \tag{61}$$

where symmetry of the integral was used and a factor of 2 was adsorbed into C_0. The substitution $\zeta = \mathrm{e}^{\mathrm{i}k}$ can be made to turn equation (61) into a contour integral around the unit disk in the ζ-plane. Denote $\zeta^* = 1/\zeta$, then it follows that

$$v_n(j) = C_0 \oint_C \left[(\zeta + \zeta^*)^n \left\{ \zeta^{j-j_0} - \left(\frac{\zeta + \zeta^* - z\zeta^*}{\zeta + \zeta^* - z\zeta} \right) \zeta^{j+j_0} \right\} \right] \frac{\mathrm{d}\zeta}{i\zeta}. \tag{62}$$

The residue theorem may be applied to this contour integral. In that case it selects the constant term (multiplied by a factor of 2π) from the Laurent series of the integrand in square brackets about $\zeta = 0$. Define the operator $CT[\cdot]$ to select this constant term, then up to an unknown constant C_0 (into which all constant factors are adsorbed), the constant term solution to the difference equation (56) is given by

$$v_n(j) = C_0 CT \left[(\zeta + \zeta^*)^n \left\{ \zeta^{j-j_0} - \left(\frac{\zeta + \zeta^* - z\zeta^*}{\zeta + \zeta^* - z\zeta} \right) \zeta^{j+j_0} \right\} \right]. \tag{63}$$

If $j = j_0 = 0$, then this should reduce to the adsorbing Dyck path partition function. C_0 may be fixed by considering this case. Since only even length paths are encountered in that model, replace n by $2n$ and expand the resulting factor $(\zeta + \zeta^*)^{2n}$ to find that

$$\begin{aligned} v_{2n}(0;0) &= C_0 CT \left[\sum_{l=0}^{2n} \binom{2n}{l} \zeta^{2n-2l} \left(\frac{z(1-\zeta^2)}{1 + (1-z)\zeta^2} \right) \right] \\ &= zC_0 \sum_{l=0}^{n} \left[\frac{2l+1}{n+l+1} \right] \binom{2n}{n+l} (z-1)^l. \end{aligned} \tag{64}$$

First taking $l = 0$, followed by $n = 0$, then shows that $v_{2n}(0,0) = zC_0 + \cdots$, and one may fix $C_0 = 1$, since the trivial Dyck path is a single vertex at the origin. The generating function of adsorbing Dyck paths may be determined by putting $j = j_0 = 0$. Multiplying equation (64) by t^{2n} and summing over n gives equation (21).

The partition function for arbitrary j and j_0 can be determined by expanding the factors in equation (63) and then selecting the constant term:

$$v_n(j; j_0) = \binom{n}{\frac{n+j-j_0}{2}} - \binom{n}{\frac{n+j+j_0}{2}} + z \sum_{l=0}^{(n-j-j_0)/2} \left[\binom{n}{\frac{n+j+j_0}{2} + l} - \binom{n}{\frac{n+j+j_0}{2} + l + 1} \right] (z-1)^l. \tag{65}$$

The first two terms count random walks on the positive integer axis, starting at j_0, and terminating at j, while avoiding the main diagonal. These are also directed paths starting at a height j_0 and terminating at a height j, and otherwise are disjoint with the main diagonal. The full generating function may be determined by multiplying equation (66) by t^n and summing over n:

$$C_e(t, z; j_0, j) = \frac{(2t)^{j+j_0}}{(1+\sqrt{1-4t^2})^{j+j_0}} \left(\frac{2z}{2 - z(1-\sqrt{1-4t^2})} \right). \tag{66}$$

Putting $j_0 = 0$ and summing over j gives the generating function of a Dyck path with a tail; it visits the main diagonal a last time and then wanders off in the square lattice. This generating function is given by

$$C_t(t, z) = \frac{z(1 - 2t + \sqrt{1-4t^2})}{(1-2t)(2 - z(1-\sqrt{1-4t^2}))} \tag{67}$$

and it was previously obtained in equation (33).

2.6. Dyck path models of adsorbing copolymers

Directed path models of adsorbing copolymers can be created by colouring vertices in the path, and then giving them separate properties. Such models are defined in reference [64], and also for self-avoiding walk models of copolymers in [47].

A linear copolymer is a linear polymer with two or more different types of monomers substituted along the polymer chain. In some cases the types of monomers along the polymer may be random, this is a *random copolymer*. If the (random) sequence of monomers are fixed along the copolymer, then the copolymer is said to be *quenched*.

There are copolymers that have a sequence of monomers that repeats periodically. Such copolymers are *periodic*, and the length of the repeating sequence is its period. An *alternating copolymer* is a periodic copolymer of period 2; it has two types of monomers that alternate in sequence along the copolymer. In some periodic copolymers the repeating sequence has the form $\left(A_1^{n_1} A_2^{m_2} \dots A_p^{m_p}\right)^*$. These are *block copolymers* of period $n_1 + n_2 + \cdots n_p$. If $p = 2$ and $n_1 = n_2$, then we have an *alternating block copolymer*.

The simplest lattice model of an adsorbing copolymer is a Dyck path with coloured vertices and with visits weighted according to colour. If the vertices of a Dyck path are labeled by $1, 2, 3, \dots$, starting from the origin, then only vertices with odd labels (called *odd vertices*) may visit the main diagonal. In other words, if the path is coloured by a sequence of colours $\chi = \langle C_1, C_2, C_3, \dots \rangle$, then the colours C_i will be placed only on the odd vertices—the even vertices will remain colourless, since they cannot interact with the main diagonal. It is generally a difficult problem to determine the generating function of a Dyck path model of a quenched copolymer, even in the cases that the copolymer has a simple structure, such as being a block copolymer.

2.6.1. Adsorbing random copolymers in the annealed ensemble. Consider a Dyck path coloured with two colours A and B, such that any odd vertex has a probability p of being colour A, and $1 - p$ to be of colour B. Simplify this model by assuming that only vertices of colour A adsorb (interacts) in the main diagonal. In the *annealed ensemble* the partition function of the Dyck path is averaged over the set of all possible colourings of the path. This model corresponds to the (rather unphysical) situation that monomers in the copolymer can change their colours (properties) randomly.

The generating function in the annealed model can be determined by noting that in every realization of the path with v visits, each visit is type A with probability p and type B with

probability $1-p$. If $w \leqslant v$ visits are of type A, and there are $c_n(v)$ Dyck paths with v visits, then the generating function is

$$C_a(t,z;p) = \sum_{n=0}^{\infty}\sum_{v=0}^{n+1}\sum_{w=0}^{v} c_n(v)\binom{v}{w}(pz)^w(1-p)^{v-w}t^n. \tag{68}$$

This may be evaluated in closed form by noting that

$$C_a(t,z;p) = \sum_{n=0}^{\infty}\sum_{v=0}^{n+1} c_v(v)(pz+1-p)^v t^n = C(t, pz+1-p) \tag{69}$$

where $C(t,z)$ is the generating function of adsorbing Dyck paths given by equation (21). Thus

$$C_a(t,z;p) = \frac{2(pz+1-p)}{2-(pz+1-p)(1-\sqrt{1-4t^2})} \tag{70}$$

is the generating function of the adsorbing Dyck path in the annealed ensemble. The radius of convergence is given by

$$t_c(z;p) = \begin{cases} \frac{1}{2} & \text{if} \quad z \leqslant 1+\frac{1}{p} \\ \frac{\sqrt{p(z-1)}}{1+p(z-1)} & \text{if} \quad z > 1+\frac{1}{p}. \end{cases} \tag{71}$$

The critical point depends on the probability by

$$z_c(p) = 1 + \frac{1}{p}. \tag{72}$$

One may explicitly compute the limiting free energy in this model, and expanding it about $z = z_c(p)$ shows again that the specific heat exponent has value $\alpha = 0$.

2.6.2. Quenched models of Dyck path copolymer adsorption. A *quenched random copolymer* is obtained when the (random) sequence of monomers is fixed along the copolymer chain. This may be modelled by a randomly coloured Dyck path with the sequence of coloured vertices fixed along the path in a particular (random) sequence. The *averaged quenched model* is that ensemble where the free energy of the model is averaged over all possible random colourings.

Let $\langle\chi_i\rangle$ be a sequence of colours (for example, each χ_i is selected from the set $\Omega = \{A, B\}$, but more colours can be included). A Dyck path is then coloured by colouring the $(2i-1)$th vertex v_{2i-1} with χ_i, where v_1 is the first vertex in the Dyck path at the origin of the square lattice. A model can be defined by letting $c_n(v, v_a|\chi)$ be the number of Dyck paths of length n coloured by the first $n/2+1$ colours in χ, and with v visits of which v_a visits are A-coloured.

The partition in such a model is

$$Z_n(z,a|\chi) = \sum_{v,v_a} c_n(v,v_a|\chi) z^v a^{v_a} \tag{73}$$

and in the limit that $n \to \infty$, the quenched limiting free energy would be defined by

$$\mathcal{F}_{qu}(z,a|\chi) = \lim_{n\to\infty}\frac{1}{n}\log Z_n(z,a|\chi) \tag{74}$$

if this limit exists[3]. It can be shown that there is a limiting free energy in the *averaged quenched model*; this is defined by

$$\mathcal{F}_{qu}(z,a) = \lim_{n\to\infty}\frac{1}{n}\langle\log Z_n(z,a|\chi)\rangle_\chi \tag{75}$$

[3] $\mathcal{F}_{qu}(z,a|\chi)$ is defined on the space of sequences $\langle\chi_i\rangle$ on the set Ω. If there are n colours, then the $\langle\chi_i\rangle$ are n-ary expansions of numbers in the interval [0, 1]. This implies that $\mathcal{F}_{qu}(z,a|\chi)$ be considered a function over a Lebesgue measure space of sequences of colourings, defining an integral over the space of colourings, from which averages such as $\langle\cdot\rangle_\chi$ over all colourings can be defined.

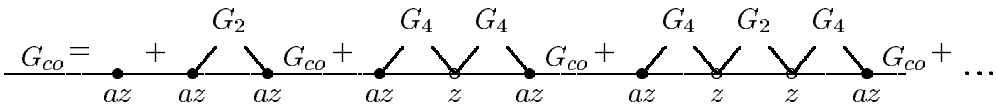

Figure 7. The Dyck path generating function of an alternating copolymer is either a single A-visit, or return for the first time to the main diagonal in an A-visit, or return for the first time to the main diagonal in a B-visit. If it returns first in a B-visit, then it could return any number of times in B-visits before a return to an A visit is obtained. Since the last vertex is an A-visit, it is guarenteed that there will be a return to an A-visit.

where $\langle\cdot\rangle$ is the average over all possible colourings χ. A proof of this is given in the appendix. It can also be shown that

$$\mathcal{F}_{qu}(z,a) = \lim_{n\to\infty} \frac{1}{n} \log Z_n(z,a|\chi) \qquad \text{for almost every colouring } \chi \tag{76}$$

so that the averaged quenched free energy is almost always equal to the quenched free energy (with respect to a uniform measure on the space of all colourings). Since $\mathcal{F}_{qu}(z,a|\chi) = \mathcal{F}_{qu}(z,a)$ a.e., it follows that the free energy model is self-averaging and that $\mathcal{F}_{qu}(z,a|\chi)$ is a measurable function on the measure space of colourings (this is [0, 1] with Lebesgue measure, since each n-ary expansion of a number $x \in [0,1]$ would give a sequence of colours in the set $\{1, 2, \ldots, n\}$). There are number of self-avoiding walk and lattice tree models of copolymers that are known to have self-averaging free energies [47, 41, 42, 67]. Self-averaging in lattice models of polymers was also discussed in [48]—in particular, conditions were set out under which self-averaging of the limiting free energy will also imply self-averaging of the energy and the specific heat of the model (these are the first two derivatives of the limiting free energy). Bounds on the extent of self-averaging in finite models of random copolymers were presented in [33].

Explicit formulae for quenched models of coloured Dyck paths are known in only a few cases. One may, for example, solve for a model with the alternating colouring $\xi = ABABABABA\ldots$. The starting point is to first find the generating function $C_4(t)$ of Dyck paths of length 0 mod 4: Since Dyck paths are counted by Catalan numbers, it follows by direct computation that

$$C_4(t) = \frac{\sqrt{2}}{\sqrt{1+\sqrt{1-16t^4}}}. \tag{77}$$

Consider now Dyck paths of length 2 mod 4 with generating function $C_2(t)$. By subtracting $C_4(t)$ from the generating function $C(t)$ (equation (19)) of Dyck paths, one obtains

$$C_2(t) = \frac{2-2\sqrt{1-16t^4}}{2+\sqrt{1-\sqrt{1-16t^4}}}. \tag{78}$$

Using the $C_4(t)$ and $C_2(t)$, it is possible to determine $C_{co}(t,z,a;\xi)$, the generating function of adsorbing Dyck paths quenched by ξ and with az generating A-coloured visits and z generating B-visits. It follows from figure 7 that

$$\begin{aligned} G_{co}(t,z,a;\xi) &= az + azt^2 G_2(t) G_{co}(t,z,a;\xi) + az^2t^4[G_4(t)]^2 G_{co}(t,z,a;\xi) \\ &\quad + az^3t^6[G_4(t)]^2 G_2(t) G_{co}(t,z,a;\xi) + \cdots, \end{aligned} \tag{79}$$

so that one may solve for $G_{co}(t,z,a;\xi)$ in term of $G_2(t)$ and $G_4(t)$:

$$G_{co}(t,z,a;\xi) = \frac{z}{1-azt^2G_2(t) - \frac{az^2t^4[G_4(t)]^2}{1-zt^2G_2(t)}}. \tag{80}$$

Consider now the case that $z = 1$, so that only A-visits interact with the main diagonal. Then the radius of convergence is given by

$$t_\xi(1,a) = \begin{cases} \frac{1}{2} & \text{if} \quad a \leqslant 2+\sqrt{2} \\ \frac{[\sqrt{\sqrt{8a^3-20a^2+16a}-4}]}{2a} & \text{if} \quad a \geqslant 2+\sqrt{2}. \end{cases} \tag{81}$$

The critical adsorption point is at

$$a_\xi = 2+\sqrt{2}. \tag{82}$$

The limiting free energy may be computed from $t_\xi(a)$, the result is that

$$\mathcal{F}_{co}(1,a;\xi) = \begin{cases} \log 2 & \text{if} \quad a \leqslant a_\xi \\ \log(\sqrt{2}a) - \log(\sqrt{(a-1)\sqrt{2a-1}}) & \text{if} \quad a > a_\xi. \end{cases} \tag{83}$$

There are more results known for other sequences [64]. Calculating the location of the critical point in quenched models remains generally an open question.

2.6.3. Adsorption of a $\{AB^{p-1}\}^*A$ coloured Dyck path. The ideas in section 2.2, and in particular the exchange relation in equation (22), may be used to find an expression for the generating function for adsorbing Dyck paths coloured by $\chi_p = \{AB^{p-1}\}^*A$, where each type of monomer interacts differently with the main diagonal. The generating function of this model is

$$C(t,z,a|\chi_p) = \sum_{n=0}^{\infty}\sum_{v,a} = c_n(v,v_a)z^v a^{v_a}t^n \tag{84}$$

where $c_n(v,v_a)$ is the number of Dyck paths of length n coloured by χ_p with v visits (of any colour) and v_a visits of colour A. Consistent with the last section, az generates A-visits, while z generate B-visits.

To determine $C(t,z,a|\chi_p)$, first define $U_p(t,z)$ to be the generating function of Dyck paths of length 0 mod $2p$, and with visits generated by z, and edges by t. Observe that $U_p(t,z)$ is given by

$$U_p(t,z) = \frac{1}{p}\sum_{j=0}^{p-1} C(\beta^j t, z) \qquad \text{where} \quad \beta = \mathrm{e}^{\mathrm{i}\pi p} \tag{85}$$

in terms of $C(t,z)$, the generating function of adsorbing Dyck paths is given by equation (21). Define $L(t,z,a|\chi_p)$ to be the generating function of Dyck paths coloured by χ_p and of length 0 mod $2p$, with visits (of any colour) generated by z, and with A-visits generated by a. By following the arguments leading to equation (22) with Dyck paths of length 0 mod $2p$ and partially coloured by χ_p, one establishes the exchange relation

$$aL(t,z,a|\chi_p)(U_p(t,z)-z) = (L(t,z,a|\chi_p) - za)U_p(t,z) \tag{86}$$

between $L(t,z,a|\chi_p)$ and $U_p(t,z)$. Solving explicitly for $L(t,z,a|\chi_p)$ gives

$$L(t,z,a|\chi_p) = \frac{zaU_p(t,z)}{za+(1-a)U_p(t,z)}. \tag{87}$$

To find an expression for the full generating function argue as follows: Each Dyck path counted by $C(t,z,a|\chi_p)$ may be factored by cutting it in its last A-visit into a Dyck path of length 0 mod $2p$, coloured by χ_p, and into a remainder of arbitrary length and with no A-visits. Thus

$$C(t,z,a|\chi_p) = L(t,z,a|\chi_p)C(t,z,0|\chi_p). \tag{88}$$

Now put $a = 1$ in this equation, and solve for

$$C(t, z, 0|\chi_p) = \frac{C(t, z, 1|\chi_p)}{L(t, z, 1|\chi_p)} = \frac{C(t, z)}{U_p(t, z)} \tag{89}$$

where it was observed that $U_p(t, z) = L(t, z, 1|\chi_p)$. Using equations (88) and (89) in equation (87), then shows that

$$C(t, z, a|\chi_p) = \frac{zaC(t, z)}{za + (1 - a)U_p(t, z)}. \tag{90}$$

The generating function $C(t, 1, a|\chi_p)$ generates walks with only A-visits adsorbing. One may also take $a \to 1/a$ and then replace $z \to a$ to obtain the generating function of adsorbing paths with the complementary colouring $\tilde{\chi}_p = \{BA^{p-1}\}^*B$ and with only the A-visits adsorbing:

$$C(t, 1, a|\tilde{\chi}_p) = C(t, a, 1/a|\chi_p). \tag{91}$$

The location of the critical adsorption point $a_c(p)$ in these models is a more challenging problem. Clearly, $a_c(1) = 2$ from equation (24), and it follows from equation (82) that $a_c(2) = z_\xi = 2 + \sqrt{2}$. It is possible to find $a_c(p)$ for the next values of p, but this soon becomes a difficult task, and no general sequence of exact values are known [64].

Instead, it is possible to develop an asymptotic expression for $a_c(p)$ [57]. There are two sources of singularities in $C(t, 1, a|\chi_p)$; namely square root singularities in $C(t, 1)$ and $U_p(t, 1)$, and simple poles whenever the denominator vanishes; this is given by solutions of

$$\frac{a}{a - 1} = U_p(t, 1). \tag{92}$$

Observe also from equations (85) and (21) that

$$U_p(t, 1) = -\frac{1}{p}\sum_{j=0}^{p-1} \frac{\sqrt{1 - 4t^2\beta^{2j}}}{2t^2\beta^{2j}} \qquad \text{where} \quad \beta = \mathrm{e}^{\mathrm{i}\pi p}. \tag{93}$$

The singularity in $U_p(t, 1)$ on the real axis is at $t = 1/2$, and this should determine the radius of convergence for $C(t, 1, a|\chi_p)$ at small values of a. For larger a, the simple poles given at values of t defined by the solution of equation (92) determines the radius of convergence, and these two sources of singularities coincides whenever $a/(a - 1) = U_p(1/2, 1)$. In other words, the critical adsorption activity is given by

$$a_c(p) = \frac{U_p(1/2, 1)}{U_p(1/2, 1) - 1}. \tag{94}$$

To find an asymptotic expression for $a_c(p)$, one must find asymptotics for $U_p(1/2, 1)$ in p, the period of the colouring.

Observe that $U_p(t, 1)$ is the generating function of Dyck paths of length 0 mod $2p$. Since Dyck paths are counted by Catalan numbers, it follows that

$$U_p\left(\frac{1}{2}, 1\right) = 1 + \sum_{n>1} \binom{2np}{np} \frac{4^{-np}}{np + 1}. \tag{95}$$

There exists an $M > 0$ such that Catalan numbers are bounded by

$$\left| \binom{2n}{n} \frac{\sqrt{\pi n^3}}{(n + 1)4^n} - \left(1 - \frac{9}{8n} + \frac{145}{128n^2}\right) \right| < \frac{M}{n^3}. \tag{96}$$

To see this, follow theorem 5.2 in chapter 5 of Flajolet and Sedgewick (or see lemma 4.4 in [57]). Substitution of this into the previous expression for $U_p\left(\frac{1}{2}, 1\right)$ shows that

$$U_p\left(\frac{1}{2}, 1\right) \sim 1 + \frac{1}{\sqrt{\pi p^3}}\left(\zeta\left(\frac{3}{2}\right) - \frac{9}{8p}\zeta\left(\frac{5}{2}\right) + \frac{145}{128p^2}\zeta\left(\frac{7}{2}\right) + O\left(\frac{1}{p^3}\right)\right). \tag{97}$$

Substitution into equation (94), then leads to

$$a_c(p) \sim \frac{\sqrt{\pi}}{\zeta\left(\frac{3}{2}\right)}p^{3/2} + \frac{9\sqrt{\pi}\zeta\left(\frac{5}{2}\right)}{8\left(\zeta\left(\frac{3}{2}\right)\right)^2}p^{1/2} + 1 + O(p^{-1/2}) \tag{98}$$

up to the first decaying term.

The analysis of this model with the complementary colouring $\tilde{\chi}_p$ colour sequence is more problematic, and remains unsolved. The generating function is

$$C(t, a, 1/a|\chi_p) = \frac{aC(t, z)}{a + (a-1)U_p(t, a)}. \tag{99}$$

There are again square root singularities present in $C(t, a)$ and $U_p(t, a)$ at $t = 1/2$. Whenever $a > 2$, there are also poles in both $C(t, a)$ and $U_p(t, a)$ at $t = \sqrt{a-1}/a$, but it can be shown that these cancel [57]. Finally, there is a curve of poles along solutions of $a + (a-1)U_p(t, a) = 0$ so that the critical point is determined by the solution of

$$a + (a-1)U_p\left(\tfrac{1}{2}, a\right) = 0. \tag{100}$$

To see all of the above, define

$$f(t, a) = \frac{a(2 - a - a\sqrt{1-4t^2})}{2(1-a)} \qquad \phi(a) = \frac{a^2}{a-1} \tag{101}$$

so that

$$C(t, a) = \frac{f(t, a)}{1 - \phi t^2} \qquad U_p(t, a) = \frac{1}{p}\sum_{p=0}^{p-1}\frac{f(t\beta^j, a)}{1 - \phi t^2\beta^2}. \tag{102}$$

Then it follows that

$$C(t, a, 1/a|\chi_p) = \frac{af(t, a)}{\frac{a-1}{p}f(t, a) + (1 - \phi t^2)\left(a + \frac{a-1}{p}\sum_{j=1}^{p-1}\frac{f(t\beta^j, a)}{1-\phi t^2\beta^2}\right)}. \tag{103}$$

Along the curve $1 - \phi t^2 = 0$ it follows that $C(t, a, 1/a|\chi_p) = ap/(a-1)$. Thus, the simple poles in $C(t, a)$ and $U_p(t, a)$ cancel. The remaining poles in $U_p(t, a)$ are zeros of $C(t, a, 1/a|\chi_p)$ and correspondingly they do not give rise to singularities either.

If $t = 1/2$ and $\phi < 1$, then the square root singularities do not cancel. The simple poles along the curve $a + (a-1)U_p(t, a) = 0$ intersects the line $t = 1/2$ to give $\tilde{a}_c(p)$, the critical point in this model. If one should naively repeat the analysis performed above to find asymptotics for $U_p(1/2, a)$, then a problem is encountered as $a \to 2^+$ along $t = 1/2$. This occurs because the poles along $a + (a-1)U_p(t, a) = 0$ approaches the branch point at $t = 1/2$ as $t \to 1/2$ and $a \to 2^+$. This is confirmed by numerical analysis [57], and this also shows that

$$\tilde{a}_c(p) \sim 2 + \frac{c_1}{p} + O\left(\frac{1}{p^{3/2}}\right) \tag{104}$$

where c_1 does not differ from 1 by more than one digit in 10^4. It is conjectured that $c_1 = 1$ [57]. The critical exponents in this model is the same as for adsorbing Dyck paths; only the location of the critical point is different.

2.7. Adsorbing Dyck paths with an area activity

A Dyck path has both its terminal vertices fixed at the main diagonal, and it encloses an area above the diagonal and below the path. The minimum area enclosed is obtained when every second vertex in the path is a visit: a path of length n will enclose a minimum area $n/4$ unit squares above the main diagonal. On the other hand, it can be checked that the maximum area that can be enclosed is $n^2/8$ unit squares. Define the *area* of a Dyck path C to be

$$\text{Area}(C) = [\text{Area under } C] - n/4. \tag{105}$$

Then $0 \leqslant \text{Area}(A) \leqslant n^2/8 - n/4$, and only the number of unit lattice squares, *completely* above the main diagonal and underneath the Dyck path, is counted as area.

Suppose that t generates length, and that the activity q generates area under the Dyck path. The generating function of Dyck paths in the length–area ensemble is $C(t, q)$, and an expression for $C(t, q)$ can be obtained by determining a functional recurrence. If a Dyck path generated by $C(t, q)$ is translated away from the main diagonal to create an excursion, then each edge in the path generates $1/2$ unit square of area. Thus, excursions with enclosed area generated by q will be counted by $t^2C(t\sqrt{q}, q)$. Dissecting a Dyck path at its first return to the main diagonal (see figure 3 and equation (20)) gives

$$C(t, q) = 1 + [t^2C(t\sqrt{q}, q)]C(t, q). \tag{106}$$

Solving for $C(t, q)$ results in the expression

$$C(t, q) = \frac{1}{1 - t^2C(t\sqrt{q}, q)}. \tag{107}$$

where $t^2C(t\sqrt{q}, q)$ generates excursions, so that $C(t, q)$ is given by a sum of powers of $[t^2C(t\sqrt{q}, q)]$, first Dyck paths that are excursions are counted, then Dyck paths composed of two excursions are counted, and so on.

Equation (107) can be iterated to give an infinite fraction representation of the generating function:

$$C(t, q) = \cfrac{1}{1 - \cfrac{t^2}{1 - \cfrac{qt^2}{1 - \cfrac{q^2t^2}{\ddots}}}} \equiv 1/1 - t^2/1 - t^2q/1 - t^2q^2/\cdots \tag{108}$$

where the last expression is short-hand for the infinite fraction. By Worpitsky's theorem [63] the infinite fraction converges if $|t^2q^n| \leqslant 1/4$ for all n. Therefore, if $t^2 \leqslant 1/4$ then the radius of convergence is $q_c(t) = 1$. For larger values of t and q small enough $C(t\sqrt{q}, q)$ will converge, but there will be a simple pole in $C(t, q)$ determined by the solution of $1 - t^2C(t\sqrt{q}, q) = 0$. Observe also that

$$C(t, q) > 1 + t^2C(t\sqrt{q}, q) \tag{109}$$

and this shows that if $1 - t^2C(t\sqrt{q}, q) \to 0$ for large enough t, then $C(t, q) \to \infty$ via a simple pole if t is big enough.

It is possible to find a solution for $C(t, q)$ as the ratio of two q-deformed exponentials. Equation (106) implies that $C(t, q) = 1 + \alpha_1t^2 + \alpha_2t^4 + \cdots$ so that only even powers of t should occur in $C(t, q)$. Make the following ansatz:

$$C(t, q) = \alpha \left[\frac{H(t^2q)}{H(t^2)} \right]. \tag{110}$$

Substitution into equation (106) and simplification gives the linear second-order functional recursion

$$\alpha^2t^2H(t^2q^2) - \alpha H(t^2q) + H(t^2) = 0. \tag{111}$$

Assuming that $H(t^2) = 1 + O(t^2)$ then implies that

$$\alpha^2 t^2 - \alpha + 1 + O(t^2) = 0. \tag{112}$$

The only choice for α that cancels the constant terms above is $\alpha = 1$; this reduces equation (111) to the following functional recursion for $H(t^2)$:

$$t^2 H(t^2 q^2) - H(t^2 q) + H(t^2) = 0. \tag{113}$$

This may be solved by assuming an infinite series solution. Substitute $\sigma = t^2$ in the above to find $[\sigma H(\sigma q^2) - H(\sigma q) + H(\sigma)] = 0$ and make the ansatz $H(\sigma) = \sum_{n \geqslant 0} \alpha_n \sigma^n$. Substitution into the recurrence shows that

$$\alpha_n = \frac{q^{2(n-1)}}{q^n - 1} \alpha_{n-1}. \tag{114}$$

Putting $\alpha_0 = 1$ and iterating this recurrence shows that

$$\alpha_n = \frac{(-1)^n q^{n(n-1)}}{\prod_{j=1}^{n} (1 - q^j)} = \frac{(-1)^n q^{n(n-1)}}{(q;q)_n} \tag{115}$$

where the q-deformed factorial defined by

$$(\sigma;q)_n = \prod_{j=1}^{n} (1 - \sigma q^{j-1}) \tag{116}$$

was used. Thus, a solution for $C(t,q)$ as a ratio of two infinite series is obtained. Since $C(t,q)$ is also a continued fraction (equation (108)), one finds that

$$C(t,q) = \frac{\sum_{n=0}^{\infty} \frac{(-1)^n q^{n^2} t^{2n}}{(q;q)_n}}{\sum_{n=0}^{\infty} \frac{(-1)^n q^{n(n-1)} t^{2n}}{(q;q)_n}} = 1/1 - t^2/1 - t^2 q/1 - t^2 q^2/\cdots \tag{117}$$

and the result is a non-trivial identity involving a ratio of infinite series on the left-hand side, and an infinite fraction on the right-hand side. The function

$$E(t^2, q) = \sum_{n=0}^{\infty} \frac{(-1)^n q^{n^2} t^{2n}}{(q;q)_n} \tag{118}$$

is the q-exponential, and $C(t,q)$ may be expressed as the ratio

$$C(t,q) = \frac{E(t^2, q)}{E(t^2/q, q)}. \tag{119}$$

This result was also mentioned in [22], and is related to the Rogers–Ramanujan identities and the fountain of coins problem [46].

Finding the limiting free energy of this model requires the determination of the radius of convergence of $C(t,q)$. This problem is unsolved, but the critical point can be determined. It was already pointed out that $C(t,q)$ converges if $q \leqslant 1$ and $t^2 \leqslant 1/4$; a result that follows from Worpitsky's theorem. Moreover, $C(t,q)$ is divergent for real $q > 1$ so that if $t^2 \leqslant 1/4$, then $q_c(t) = 1$. The essential singularity in $E(t^2, q)$ above determines $q_c(t)$ in this regime.

Setting $q = 1$ in equation (117) and solving explicitly gives $C(t,1)$ in equation (19). This gives the point $(t,q) = (1/2, 1)$ as a candidate for a critical point. If $t = 1/2$ then the infinite fraction reduces to

$$C(1/2, q) = \cfrac{1}{1 - \cfrac{1/4}{1 - \cfrac{q/4}{1 - \frac{q^2/4}{1 - \cdots}}}} \tag{120}$$

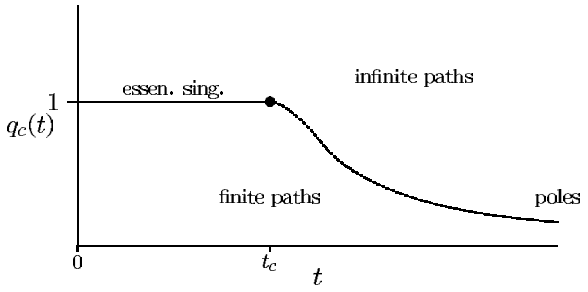

Figure 8. The radius of convergence $q_c(t)$ for inflating Dyck paths. The critical point is $t_c = 1/2$. For $t < 1/2$, the radius of convergence of $q_c(t)$ is determined by an essential singularity in $C(t, q)$ as $q \nearrow 1$. Along the critical curve $q_c(t)$, for $t > 1/2$, the radius of convergence is determined by a simple pole given by the solution of $1 = t^2 C(t\sqrt{q}, q)$.

which have an essential singularity at $q = 1$, as may be observed from equation (119) (since $(q; q)_n = 0$ for all n if $q = 1$).

The q-exponential (equation (118)) is absolutely convergent if $|q| < 1$. Thus $E(t^2, q)$ is an analytic function if $|q| < 1$, and $C(t, q)$ is a meromorphic function in the unit circle $|q| < 1$ (it is the ratio of two holomorphic functions). It follows that singularities in $C(t, q)$ are given in this domain by roots of $E(t^2/q, q)$. For $t^2 > 1/4$ there is a singularity along the curves $1 = t^2 C(t\sqrt{q}, q)$. In this case, $q_c(t) < 1$, and since it was noted in equation (109) that $C(t, q) > 1 + t^2 C(t\sqrt{q}, q)$, it follows that the radius of convergence of $C(t, q)$ is given by the solution of $t^2 C(t\sqrt{q}, q) = 1$, corresponding to a zero of $E(t^2/q, q)$. This is a curve of simple poles in the tq-plane. In other words

$$q_c(t) \begin{cases} =1 & \text{if} \quad t \leqslant \frac{1}{2} \\ <1 & \text{if} \quad t > \frac{1}{2}. \end{cases} \tag{121}$$

A plot of $q_c(t)$ is similar to that of $t_c(z)$ in figure 2, this is shown in figure 8.

The Dyck path with area and perimeter activities are said to be a model of *inflating* Dyck paths. This term refers to the ratio of area to perimeter in different phases. Inverting the function $q_c(t)$ to $t_c(q)$ gives a limiting free energy as a function of the area activity. One may check that $q_c = 1$ is the critical point, and the derivative of $\mathcal{F}(q)$ to $\log q$ is positive if $q < 1$. Thus, the density of perimeter edges to area is positive if $q < 1$. If $q > 1$, then $\mathcal{F}(q) = \infty$, and by first noting that $t_c(q) = 0$ if $q > 1$, one may conclude that the ratio of perimeter edges to area is zero in this regime. That is, the Dyck path is inflated like a blister on the main diagonal.

This model is related to partition polygons (see for example [60]). In this model, the area–perimeter generating function is given by

$$G_p(t, q) = \sum_{n=0}^{\infty} \frac{t^{2n}}{(t^2 q; q)_n} = \sum_{n=0}^{\infty} \frac{t^{4n} q^{n^2}}{(t^2 q; q)_n^2}. \tag{122}$$

The phase diagram in this model is simpler; the phase boundary can easily be seen to be given by

$$q_c(t) = \begin{cases} 1 & \text{if} \quad t \leqslant 1 \\ \frac{1}{t^2} & \text{if} \quad t > 1. \end{cases} \tag{123}$$

The singularity along $q_c(t) = 1$ is an accumulation of simple poles along the curves $t^{2m} q = 1$ for $m = 1, 2, \ldots$ and is thus an essential singularity. For $t > 1$ the phase boundary is a simple

pole. It can be checked that the transition at $t_c = 1$ is similarly an inflation if the partition polygon [54]. Results for an inflating transition have also been obtained in area–perimeter models of staircase polygons, and a variety of other convex and partially convex models of lattice polygons, and partially directed walks [7, 9, 12, 53].

2.7.1. Adsorbing and inflating Dyck paths. Dyck paths may be studied in an adsorbing and inflating model if an activity z conjugate to the number of visits in the main diagonal is introduced in the model. Such a Dyck path is either a single visit, or consists of an excursion (with an area activity and no visits), followed by a Dyck path with both an area and a visit activity. The functional recurrence for the perimeter–area–visit generating function $C(t, q, z)$ is

$$C(t, q, z) = z + [zt^2 C(t\sqrt{q}, q)]C(t, q, z). \tag{124}$$

This may be solved by first writing

$$C(t, q, z) = \frac{z}{1 - zt^2 C(t\sqrt{q}, q)} \tag{125}$$

and from this an infinite fraction solution may be developed for $C(t, q, z)$:

$$C(t, q, z) = z/1 - zt^2/1 - t^2q/1 - t^2q^2/1 - t^2q^3/1 - \cdots. \tag{126}$$

The radius of convergence in the q-plane may be determined by applying Worpitsky's theorem: In this case, if both $|zt^2| \leqslant 1/4$ and $|t^2q^m| \leqslant 1/4$, $m = 1, 2, \ldots$, then $C(t, q, z)$ is convergent in the q-plane. Singularities may arise if either z is increased, resulting in a simple pole in $C(t, q, z)$, or t is increased; to see this, arguments similar to those in section 2.7 may be used. Putting $z = 1$ reduces the model to inflating Dyck paths encountered in the last section, while if $q = 1$ the model of adsorbing Dyck paths in section 2.2 is obtained.

Consider first the tz-plane: observe that $q_c(t, z) \leqslant 1$ for all values of t and z. If $t \leqslant 1/2$ then it follows that for small enough values of z

$$C(t, 1, z) = \frac{2z}{2 - z(1 - \sqrt{1 - 4t^2})} \qquad \text{if } t \leqslant 1/2 \text{ and } z \text{ is small.} \tag{127}$$

This is the adsorbing Dyck path generating function, first derived in equation (21) (see figure 3). A simple pole develops in $C(t, 1, z)$ as

$$z \nearrow z_c(t) = \frac{(1 + \sqrt{1 - 4t^2})}{2t^2} = \frac{2}{1 - \sqrt{1 - 4t^2}}. \tag{128}$$

This phase with $t < 1/2$ and $z < z_c(t)$ is a phase of desorbed Dyck paths. In this regime, $q_c(t, z) = 1$, and it corresponds to an essential singularity in $C(t, q, z)$; as one would see by using the same arguments as for $C(t, q)$ above (this also corresponds to the line of essential singularities in figure 8).

In the event that $t < 1/2$ and $z > z_c(t)$, then a simple pole determines $q_c(t, z)$; this can be computed by solving $zt^2 C(t\sqrt{q}, q) = 1$. Since Worpitsky's theorem bounds $2/3 \leqslant C(t\sqrt{q}, q) \leqslant 2$ for values of q within the radius of convergence of the infinite fraction, this shows that $z_c(t) \geqslant 2$ if $t \leqslant 1/2$, consistent with equation (128) above. This is a phase of adsorbed paths.

Lastly, if $t > 1/2$ then a simple pole determined by $zt^2 C(t\sqrt{q}, q) = 1$ determines the radius of convergence, for any $z > 0$. This is a phase of adsorbed paths, with a positive density of visits in the main diagonal. This phase is indistinguishable from the phase with $t < 1/2$ and $z > z_c(t)$. In other words, there are two phases in this model, a desorbed-inflated and an adsorbed-deflated phase.

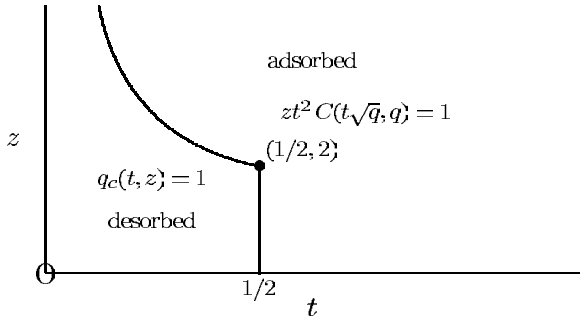

Figure 9. The phase diagram of adsorbing Dyck paths in the zt-plane. For small z and t the radius of convergence of $C(t, q, z)$ is $q_c(t, z) = 1$ and this is an essential singularity in $C(t, q, z)$ that corresponds to a phase of desorbed Dyck paths. Increasing z so that $z > z_c(t) = (1 + \sqrt{1 - 4t^2})/2t^2$, or $t > 1/2$, takes the model to a phase of adsorbed Dyck paths with radius of convergence determined by the solution of $zt^2C(t\sqrt{q}, q) = 1$.

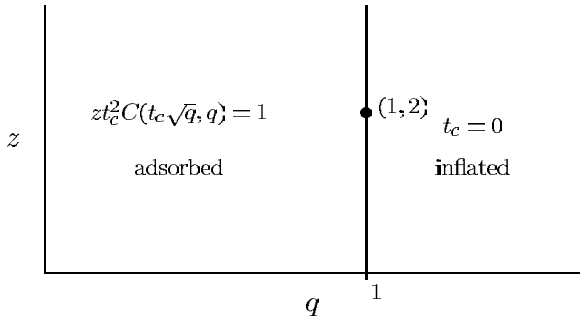

Figure 10. The phase diagram of adsorbing and inflating Dyck paths in the qz-plane. For $q < 1$ the radius of convergence of $C(t, q, z)$ is determined by $zt^2C(t\sqrt{q}, q) = 1$, giving a simple pole in $C(t, q, z)$ and defining an adsorbed phase. If $q = 1$, then the model has generating function given by equation (127), with a critical adsorption activity $z_c = 2$. If $q = 0$, then $C(t, 0, z) = z/(1-zt^2)$, so that there is a simple pole at $t_c(0, z) = 1/\sqrt{z}$. Thus, the Dyck path is adsorbed for all values of $z > 0$ if $q = 0$. The path is trivially desorbed for all $z = 0$. If $q > 1$, then the path is inflated (and desorbed) for all $z \geqslant 0$ and moreover, $t_c = 0$.

An alternative point of view is presented if the qz-plane is considered. The radius of convergence in that case is $t_c(q, z)$ and the limiting free energy (per edge) is $-\log t_c(q, z)$. The infinite fraction $C(t\sqrt{q}, q)$ is divergent if $q > 1$ for every $t > 0$, so that $t_c(q, z) = 0$ for all $z > 0$ and $q > 1$. This is a phase of inflated (and desorbed) Dyck paths. Putting $q = 1$ gives equation (127), so that there is a critical point at $z_c = 2$. In particular, if $z < 2$, then there is a branch point singularity in $C(t, 1, z)$ at $t = 1/2$, and if $z > 2$ then a simple pole appears in $C(t, 1, z)$ at $t_c = \sqrt{z - 1}/2$.

Consider now the case that $q < 1$. If $q = 0$, then one may check that $C(t, 0, z) = 1/(1 - zt^2)$ with the result that $t_c(z) = 1/\sqrt{z}$ in the qz-plane. This is analytic in z, except at $z = 0$, so that the adsorption transition takes place at $z = 0$. If $0 < q < 1$ then $t_c(q, z)$ are determined by a simple pole in $C(t, q, z)$, when $zt^2C(t\sqrt{q}, q) = 1$. This is an adsorbed (and deflated) phase. The phase diagram is illustrated in figure 10. By Worpitsky's theorem, $2/3 \leqslant C(t, q) \leqslant 2$ inside its radius of convergence. In either case, this shows that $t_c(q, z) \sim 1/\sqrt{2}z$ asymptotically, for all $q < 1$. If $q = 1$, then the path is desorbed for $z < 2$ and adsorbed for $z > 2$. There may be a phase boundary joining $z = q = 0$ and $(z = 2, q = 1)$

separating adsorbed and desorbed phases as stated in [35]. However, a partially directed model has no such boundary [49], and the path may be adsorbed (and deflated) with an adsorption transition at $z = 0$ (where the path is trivially desorbed).

3. Statistical mechanics of Dyck paths

In section 2 a variety of models of adsorbing and inflating Dyck paths were considered. Generating functions were obtained, and via equation (8) the limiting free energies of these models were determined by finding the radius of convergence ($t_c(z)$ or $q_c(t)$) of the generating functions as a function of activities z or t. The limiting free energy, $\mathcal{F}(z)$, was determined per unit length or per unit area, and so is a density. Derivatives of $\mathcal{F}(z)$ are the energy density and the specific heat (equation (4)).

Scaling laws for these thermodynamic quantities introduced a scaling exponent α in equations (5) and (6). The exponent α describes the shape of the specific heat (or of the limiting free energy) close to the critical point; and since these are related to the radius of convergence of the generating function via equation (8), one would suppose that it is also related in some way to the generating function and in particular to the shape of the critical curve $t_c(z)$ close to the critical point.

There is more to this, and a full physical picture only emerge from the theory of *tricritical scaling* [39, 11]. The generating functions typically have phase diagrams such as in figures 2 and 8. In these cases a non-analytic point in the critical curve $t_c(z)$ (or $q_z(t)$) is identified as a critical point in the thermodynamic sense. This point is also present in the limiting free energy, and in that instance is by definition a critical point that separates two thermodynamic phases, since it is a non-analyticity in the free energy $\mathcal{F}(z)$. The interesting fact in figures 2 and 8 is that the nature of the singularity in the generating function also changes at the critical point. In figure 2 it changes from a branch point to a pole, and in figure 7 from an essential singularity to a pole. The singularity in the critical curve at the critical point may be yet different again. This suggests that there should be a general theory for the description of critical behaviour that relies on the analysis of both the nature of the singularities in the generating function, as well as the shape of the critical curve close to the critical point. This general theory forms the framework that describes tricritical and multicritical points.

The partition function and limiting free energy defined in equations (1) and (3) is the basic starting point. Since the energy density $\mathcal{E}(z)$ is finite, and is asymptotic to a number $\mathcal{E}$ (as $\log z \to \infty$), it is not unreasonable to suppose that

$$\mathcal{F}(z) \sim \mathcal{S} + \mathcal{E} \log z. \tag{129}$$

If one interprets $\log z$ as proportional to inverse temperature, then one may call $\mathcal{S}$ (or its negative) the *limiting entropy* of the model.

The limiting free energy $\mathcal{F}(z)$ is a convex function of $\log z$. This follows by application of the Cauchy–Schwartz inequality to the partition function

$$\begin{aligned} Z_n(z_1)Z_n(z_2) &= \sum_{m_1} h_n(m_1) z_1^{m_1} \sum_{m_2} h_n(m_2) z_2^{m_2} \\ &\geqslant \left(\sum_{m} h_n(m) [\sqrt{z_1 z_2}]^m \right)^2 \\ &= (Z_n(\sqrt{z_1 z_2}))^2. \end{aligned} \tag{130}$$

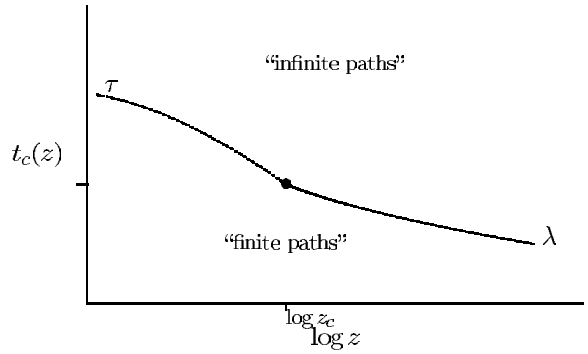

Figure 11. The generic phase diagram of a two parameter model of paths with generating function $C(t, z)$. The critical curve is given by $t_c(z)$, and it separates the diagram into a phase of 'infinite paths' and a phase of 'finite paths'. The nature of the singularity in $C(t, z)$ changes along $t_c(z)$ from a more complicated to a simpler singularity as the critical point (denoted by •) at $z = z_c$ is passed. For example, an essential singularity may change into a branch point or a pole, or a branch point may change into a pole. Critical points of this nature are *tricritical points*. The influence of the tricritical point is felt in the phase of finite paths in the *tricritical scaling region* close to the tricritical point. The tricritical point • separates the critical curve into τ-curve and a λ-curve: the τ-curve is that part of $t_c(z)$ with the more complex singularity in $C(t, z)$, while the λ-curve corresponds to the part of $t_c(z)$ corresponding to simpler singularities (poles) in $C(t, z)$.

Take logarithms of this, divide by n, to see that

$$\frac{1}{n}\log Z_n(z_1) + \frac{1}{n}\log Z_n(z_2) \geqslant \frac{2}{n}\log Z_n(\sqrt{z_1 z_2}) \tag{131}$$

and thus $[\log Z_n(z)]/n$ is a convex function of $\log z$ for each $n > 0$. Taking $n \to \infty$ in the last inequality shows that $\mathcal{F}(z)$ is the limit of a sequence of functions convex in $\log z$:

$$\mathcal{F}(z_1) + \mathcal{F}(z_2) \geqslant 2\mathcal{F}(\sqrt{z_1 z_2}). \tag{132}$$

It follows that if $\mathcal{F}(z)$ exists, then it is convex in $\log z$. Moreover, whenever $\mathcal{F}(z)$ is finite in $(0, \infty)$, then its right and left derivatives exists everywhere in $(0, \infty)$, and they are non-decreasing functions of $\log z$. Further, $\mathcal{F}(z)$ is also continuously differentiable almost everywhere, and wherever the derivative exists, it is given by $\mathcal{E}(z) = \lim_{n\to\infty}\left[\frac{\mathrm{d}F_n(z)}{\mathrm{d}\log z}\right]$ where $F_n(z) = [\log Z_n(z)]/n$; see equation (4).

The specific heat exponent α describes the nature of the critical point in $\mathcal{F}(z)$. The range of values $\alpha > 1$ seems to be ruled out by convexity in equation (132). If $\alpha = 1$, then there is a cusp in the specific heat, and a jump discontinuity in the energy density in equation (4). Such transitions are *first order*. Values of $\alpha < 1$ corresponds to *continuous transitions*; and in particular, the energy density $\mathcal{E}(z)$ changes continues through the critical point.

3.1. Tricriticality

The generic phase diagram of the grand potential $\log C(t, z)$ in a two parameter model is given in figure 11. This phase diagram is similar to those of the models in figures 2 and 8. A critical curve (radius of convergence of $C(t, z)$) $t_c(z)$ separates two phases; one is a phase of 'finite paths', where $C(t, z)$ is finite, and its value is determined primarily by paths of finite length. The second phase is one of 'infinite paths'; in this regime, $C(t, z)$ is itself divergent, as paths of arbitrary length makes non-vanishing contributions.

The general tricritical phase diagram are found in models with two external fields, or in the context here, with three parameters. The models considered here have in general two

parameters with generating functions $C(t, z)$; in such situations the tricritical phase diagram collapses to the generic phase diagram in figure 11.

In the classical description of tricriticality, the critical curve $t_c(z)$ is assumed to be differentiable in a neighbourhood of the tricritical point. The tricritical point separates the critical curve $t_c(z)$ into a τ-curve and a λ-curve; the τ-curve corresponds to the more complex singularities in $C(t, z)$ (essential singularities or branch points), while the λ-curve corresponds to simpler singularities in $C(t, z)$. These meet in the tricritical point.

In the general tricritical phase diagram, the τ-curve is a curve of triple points, and this is also the locus of common meeting points of three critical surfaces of (usually) first-order transition separating three phases. The curve of triple points ends in the tricritical point, where boundaries of the critical surfaces meet; the λ-curve is the boundary of one of these surfaces [39].

The shape of the critical curve in the vicinity of the tricritical point is implicated in the phenomonological description of tricriticality. Suppose that $t_\tau(z)$ and $t_\lambda(z)$ are the τ and λ parts of the critical curve $t_c(z)$. Expanding these about the tricritical point gives

$$\begin{aligned} t_\tau(z) &= t_c(z_c) - a_\lambda(z - z_c) - b_\tau(z_c - z)^{\psi_\tau} \\ t_\lambda(z) &= t_c(z_c) - a_\lambda(z - z_c) - b\lambda(z - z_c)^{\psi_\lambda}. \end{aligned} \tag{133}$$

The exponents ψ_τ and ψ_λ are *shift-exponents*, and they determine the shape of the critical curves close to the tricritical point. In some models, the τ-curve is linear, in which case one may assume that $b_\tau = 0$ and ψ_τ is not defined. Such models are said to be *asymmetric*.

There is a set of natural coordinates (s, g) that may be used to describe the shape of $t_\tau(z)$ and $t_\lambda(z)$ close to the tricritical point. Choose the s-axis tangent[4] to the critical curve $t_c(z)$ at $z = z_c$, and the g-axis transverse to the critical curve at the tricritical point. Appropriate definitions for the s and g coordinates might be made by considering equations (133). Choosing $s = z - z_c$, and $g = t_\lambda(z_c) - t - a_\lambda s$, reduce the expressions for the τ and λ-curves to

$$g_\tau(s) = b_\tau|s|^{\psi_\tau} \qquad g_\lambda(s) = b_\lambda s^{\psi_\lambda}. \tag{134}$$

If $g = 0 = t_\lambda(z_c) - t - a_\lambda s$, then the s-axis is described; it is tangent to the critical curve $t_\lambda(z)$ at $z = z_c$. If $s = 0$, then it follows that $g = t_\lambda(z_c) - t$, and the g-axis is transverse to the critical curve $t_\lambda(z)$ at $z = z_c$. Plotting the critical curve $t_c(z)$ in the (s, g)-plane gives figure 12.

The generating function $G(t, z)$ is singular along the critical curve in figure 12. Along the τ-curve, the singularity may be an essential singularity or a branch point singularity, and this gives way to a simpler singularity, such as a pole, along the λ-curve. We may make a stronger assumption than this: namely that $G(t, z)$ is finite along the τ-curve and that the restriction of $G(t, z)$ to the τ-curve is an analytic function of z. This implies that the transition to the infinite path phase is discontinuous along the τ-curve, consistent with the notion that this is a first-order phase transition.

Along the λ-curve $G(t, z)$ is assumed to have a continuous transition to the infinite phase. This implies a continuous first derivative of $G(t, z)$; that may be interpreted as evidence for a simpler singularity (such as a pole or a branch point) in $G(t, z)$ along the λ-curve. With the g-axis as oriented in figure 12, the following scaling assumptions are made for $G(t, z)$: Assume that the singular parts of the generating function $G(t, z)$ scale as

$$G(t, z) \sim A_\tau(t - t_\tau(z))^{2-\alpha_-} \qquad \text{along the } \tau\text{-curve} \tag{135}$$

$$G(t, z) \sim A_\lambda(t - t_\lambda(z))^{2-\alpha_+} \qquad \text{along the } \lambda\text{-curve.} \tag{136}$$

[4] In some models the derivative to the critical curve does not exist at the tricritical point. In those models the s-axis should be chosen tangent to the λ curve at the tricritical point.

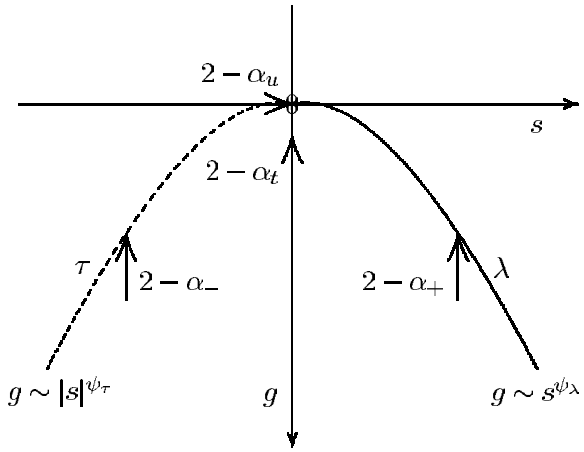

Figure 12. The tricritical phase diagram in the (s, g)-plane. The tricritical region is shaded, and the scaling assumptions of the generating function is indicated around the tricritical point, and along the τ and λ curves.

The exponents α_- and α_+ describe the nature of the singularity in $G(t, z)$ along the critical curve. The inclusion of the factor 2 in the exponents is for historical reasons, and in some sources the exponents are replaced by

$$\gamma_- = \alpha_- - 2 \qquad \text{and} \qquad \gamma_+ = \alpha_+ - 2. \tag{137}$$

The assumptions above also ignored a 'background' analytic contribution to the generating function. In models that $G(t, z)$ exhibit an essential singularity along the τ-curve, the exponent α_- does not exist.

The scaling of $G(t, z)$ in the vicinity of the tricritical point in figure 12 is described by the introduction of a *tricritical exponent* α_t:

$$G(t, z) \sim A_t g^{2-\alpha_t} \qquad \text{along the } g\text{-axis, as } g \to 0^+. \tag{138}$$

Along the τ-curve $G(t, z)$ was assumed to be analytic, but this breaks down at the tricritical point: the assumption is that

$$G(t, z) \sim A_u |s|^{2-\alpha_u} \qquad \text{along the } \tau\text{-curve, as } |s| \to 0^+. \tag{139}$$

The behaviour of $G(t, z)$ as expressed in these assumptions must be reconciled at the tricritical point. The assumption that

$$G(t, z) \approx A_t g^{2-\alpha_t} f(g^{-\phi} s) \tag{140}$$

where $f(0) = 1$ recovers equation (138). The exponents $\gamma_t = 2 - \alpha_t$ and $\gamma_u = 2 - \gamma_u$ are often introduced instead. This assumption also implies that the shape of the λ-curve close to the tricritical point is invariant under rescaling of the coordinates by $g \to Ag$ and $s \to A^\phi s$. Assuming that $f(-x) \sim x^u$ as $x \to 0^+$, and comparing this to equation (139) shows that $u = 2 - \alpha_u$, so that by equation (140) $2 - \alpha_t = \phi(2 - \alpha_u)$ and this gives the relation

$$\phi = \frac{2 - \alpha_t}{2 - \alpha_u}. \tag{141}$$

In terms of the exponents γ_t and γ_u, this is the same as $\phi = \gamma_t / \gamma_u$. The exponent ϕ is the *crossover* exponent; it describes the crossover behaviour of $G(t, z)$ from the g to the s-axis as the tricritical point is approached.

Along the λ-curve the singular part in $G(t, z)$ is given by equation (136)—this implies that the argument of the tricritical scaling function $f(x)$ in equation (140) cannot grow unbounded along this part of the critical curve. In other words, $g^{-\phi}s \approx$ constant along the λ-curve, and this shows that $g_\lambda(s) \approx b_\lambda s^{1/\phi}$. Comparison to equation (134) then shows that

$$\psi_\lambda = 1/\phi. \tag{142}$$

The shift-exponent is controlled by the shape or geometry of the λ-curve close to the critical point, and this also determines the value of the crossover exponent.

A similar analysis can be performed along the τ-curve; and in some cases it is found that $\psi_\tau = \psi_\lambda = 1/\phi$. These are the *symmetric* models. Also observe that equation (140) may be written as

$$G(t, z) \approx A_g s^{2-\alpha_u} f_0(gs^{-1/\phi}) \tag{143}$$

so that if derivatives to g are taken, then

$$\frac{\partial^n G(t, z)}{\partial g^n} \sim A_g^{(n)} s^{2-\alpha_u-n/\phi} f_0^{(n)}(gs^{-1/\phi}). \tag{144}$$

These derivatives have exponents separated by $1/\phi = \Delta$, and Δ is the *gap-exponent*. In some models it is more efficient to estimate the gap exponent in order to obtain ϕ.

3.2. Finite size scaling

The convergence of the free energy $F_n(z) = [\log Z_n(z)]/n$ to the limiting free energy $\mathcal{F}(z)$ in equation (3) introduces the notion of *finite size scaling*. The basic assumption is that the curves $F_n(z)$ are all rescaled images of the same curve about $z = z_c$. Hence, assume that $F_n(z)$, and thus the partition function $Z_n(z)$, is a function of a single variable $n^{\phi_c}(z - z_c)$, where ϕ_c is the *finite size crossover exponent* that controls the rescaling of the z-axis with n. In some respect the development of finite size scaling is similar to that of scaling of the generating function. The two scaling fields are $s = z - z_c$ and $1/n$.

The partition function $Z_n(z)$ is generated by the generating function $G(t, z)$ as in equation (7). The scaling assumptions for $G(t, z)$ in equations (136) and (140) suggest that appropriate assumptions for the scaling of $Z_n(z)$ is

$$Z_n(z) \approx \begin{cases} B_+ n^{\alpha_+-3}[t_\lambda(z)]^{-n} & \text{along the } \lambda \text{ curve} \\ B_t n^{\alpha_t-3}[t_\lambda(z_c)]^{-n} & \text{at the tricritical point} \\ B_- n^{\alpha_--3}[t_\tau(z)]^{-n} & \text{along the } \tau\text{-curve.} \end{cases} \tag{145}$$

However, $Z_n(z)$ should be a function of the combined variable $n^{\phi_c}s$, and so one may introduce a scaling function $h(x)$ so that

$$Z_n(z) \approx h(n^{\phi_c}s)n^{\alpha_t-3}[t_\tau(z)]^{-[n^{\phi_c|s|}]^{1/\phi_c}}. \tag{146}$$

In this case, by equation (145) the scaling function $h(x)$ must have asymptotic behaviour given by

$$h(x) \sim \begin{cases} B_\lambda x^{(\alpha_+-\alpha_t)/\phi_c} & \text{as} \quad x \to \infty \\ B_\tau |x|^{(\alpha_--\alpha_t)/\phi_c} & \text{as} \quad x \to -\infty. \end{cases} \tag{147}$$

In models that the path collapses to a compact shape, an entropic contribution to the free energy should come from (local) fluctuations in the surface of the compact object. The size of this contribution should be proportional to the total surface area which grows as $n^{(d-1)/d}$ in d dimensions. Consequently, a factor of the form $\mu_s^{n^\sigma}$ should appear in the scaling form of

$Z_n(z)$ along the τ-line in some models, where $\sigma = (d-1)/d$. Such a surface term is known to contribute in models such as percolation [50].

Simplify the above assumptions by putting $\mu_\lambda = 1/t_\lambda(z)$, $\mu_\tau = 1/t_\tau(z)$, and by adsorbing all factors, except n^{α_*-3} into the scaling function $h(x)$. Then

$$Z_n(z) \approx \bar{h}(n^{\phi_c}s)n^{\alpha_t-3} \tag{148}$$

where

$$\bar{h}(x) \approx \begin{cases} B_\lambda x^{(\alpha_+-\alpha_t)/\phi_c}\mu_\lambda^{x^{1/\phi_c}} & \text{as} \quad x \to \infty \\ \text{constant} & \text{if} \quad x = 0 \\ B_\tau |x|^{(\alpha_--\alpha_t)/\phi_c}\mu_s^{|x|^{\sigma/\phi_c}}\mu_\tau^{|x|^{1/\phi_c}} & \text{as} \quad x \to -\infty. \end{cases} \tag{149}$$

The scaling of the limiting free energy can be determined from equation (148) by taking logarithms and dividing by n. For large n the surface contribution is only important if $\mu_\tau = 1$, and the result is that

$$F_n(z) \approx \frac{1}{n}\mu(n^{\phi_c}s) \tag{150}$$

where

$$\mu(x) \approx \begin{cases} x^{1/\phi_c} & \text{as} \quad x \to \infty \\ |x|^{\sigma/\phi_c} & \text{if} \quad x \to -\infty \quad \text{and} \quad \mu_\tau = 1 \\ |x|^{1/\phi_c} & \text{if} \quad x \to -\infty \quad \text{and} \quad \mu_\tau > 1. \end{cases} \tag{151}$$

Along the λ-curve, where $s > 0$ one may expect that

$$\mathcal{F}(z) \sim C_t s^{1/\phi_c} \qquad \text{as} \quad s \to 0^+ \tag{152}$$

and here the analytic contributions and other non-analyticities that are dominated by the behaviour above are neglected. In equation (6) the scaling of the limiting free energy is given in terms of the specific heat exponent α. Comparison to the above shows that

$$2 - \alpha = \frac{1}{\phi_c}. \tag{153}$$

This is a hyperscaling relation that establishes a connection between the thermodynamic scaling of the specific heat in equation (5) and the finite size scaling of the partition function.

Observe that $t_c(z) = \mathrm{e}^{-\mathcal{F}(z)}$, and so $g_\lambda(s) \sim t_c(z) \sim 1 - \mathcal{F}(z) + \cdots \sim (z - z_c)^{2-\alpha}$ close to the critical point along the λ-curve by equation (6). By equations (134) and (142) it follows that

$$2 - \alpha = \psi_\lambda = 1/\phi = 1/\phi_c. \tag{154}$$

Hence $\phi = \phi_c$, and this connects the scaling of the generating function with the scaling of the partition function. It follows that $\alpha = 1$ implies that $\phi = 1$, so that $\phi = 1$ is consistent with a first-order transition in the model.

3.3. Homogeneity of the generating function

Underlying homogeneity is an assumption of scale invariance. In a system undergoing a continuous phase transition, it is assumed that there is only one length scale determined by the correlation length—the system would be invariant under a spatial dilation followed by a rescaling of the unit length to compensate for the dilation. Since the correlation length is dependent on the fields g and s, changes in these may be considered equivalent to a dilation of

space. The field g approaches zero as the tricitical point is approached, while the correlation length $\xi(g)$ diverges: Fix $s = 0$ and assume that

$$\xi(g) \simeq g^{-\nu_t} \tag{155}$$

where ν_t is the *tricritical metric exponent* describing the divergence of $\xi(g)$ as the tricritical point is approached.

Generally, rescaling of the fields g and s under a rescaling of space by a factor of σ may be controlled by two exponents y_g and y_t by assuming that

$$g \to \sigma^{y_g} g \qquad s \to \sigma^{y_t} s. \tag{156}$$

In other words, changes in g are compensated by changes in σ through $\sigma = g^{-1/y_g}$, and similarly for s. In the vicinity of the tricritical point, σ must scale with the correlation length (since that sets the scale). In other words, comparison with equation (155) shows that one should have

$$y_g = 1/\nu_t. \tag{157}$$

Homogeneity is a mathematical assumption about the behaviour of the generating function $G(t, z)$ close to criticality. The singular part of the generating function $G(t, z)$, in the coordinates (g, s), $G_s(g, s)$, is assumed to rescale under a dilation of space by a factor of σ in d dimensions as

$$G_s(g, s) \approx \sigma^{-d} G_s(\sigma^{y_g} g, \sigma^{y_t} s). \tag{158}$$

Assume that $\sigma > 1$ and that y_g and y_t are positive exponents. One may eliminate s in the above by putting $\sigma \simeq g^{-1/y_g}$ to obtain

$$G_s(g, t) \simeq g^{\mathrm{d}\nu_t} G_s(c, g^{-y_t/y_g} s) \tag{159}$$

where c is a constant, and where s is kept fixed. Since $G_s(g, s)$ is the singular part of the generating function, this may now be compared to equation (140) to note that

$$2 - \alpha_t = \mathrm{d}\nu_t \qquad \phi = y_t/y_g. \tag{160}$$

One may apply similar arguments to show that

$$2 - \alpha_u = d/y_t. \tag{161}$$

Since $\phi = y_t/y_g = y_t\nu_t$, $1/\nu_t$ can be interpreted as a fractal dimension; this also follows from equation (154) where $2 - \alpha = 1/(y_t\nu_t)$. This relates the exponent y_t to ϕ via the fractal dimension $1/\nu_t$, and it explains the use of the term 'hyperscaling relation' to describe equation (154); the dimensionality of the model enters (implicitly) via the exponent $1/\nu_t$.

It is possible to determine the scaling of generating function in a number of models discussed in section 2. For example, the model of adsorbing Dyck paths has generating function in equation (21). The critical point is at $(t, z) = (1/2, 2)$ so that the scaling fields $s = 2 - z$ and $g = 1 - 4t^2$ can be chosen. In this case it follows that

$$C(t, z) = \frac{2z}{2 - z(1 - \sqrt{1 - 4t^2})} = \frac{2z}{s(1 + zs^{-1}\sqrt{g})} = \frac{2z}{\sqrt{g}(z + s\sqrt{g}^{-1})}. \tag{162}$$

Comparison to equation (140) or to equation (143) shows that the scaling exponents can be identified. In particular, $2-\alpha_t = -1/2$ and $2-\alpha_u = -1$ while $\phi = 1/2$, so that equation (141) is confirmed for this model. The results obtained for more generating functions are given in tables 1 and 2. In the case of inflating Dyck paths the description is incomplete: there is an essential singularity at the critical point and the exponent $2 - \alpha_t$ seems to be undefined. The crossover exponent $\phi = 1$ in that model was determined by applying the method of dominant balance [58].

Table 1. Scaling of generating functions.

Equation	GF	s	g	Scaling forms
(11)	$g(t,z)$	$1-2z$	$1-t$	$\frac{1}{g^2(1-tsg^{-1})} = \frac{1}{s^2((gs^{-1})^2-t(gs^{-1}))}$
(21)	$C(t,z)$	$2-z$	$1-4t^2$	$\frac{2z}{\sqrt{g}(z+s\sqrt{g}^{-1})} = \frac{2z}{s(1+zs^{-1}\sqrt{g})}$
(30)	$D(t,z)$	$1-z$	$1-4t^2$	$\frac{z}{\sqrt{g}(z+s\sqrt{g}^{-1})} = \frac{z}{s(1+zs^{-1}\sqrt{g})}$
(33)	$C_t(t,z)$	$2-z$	$1-2t$	$\frac{z(\sqrt{g}+\sqrt{1+2t})}{g(s\sqrt{g}^{-1}+z\sqrt{1+2t})} = \frac{z(\sqrt{g}+\sqrt{1+2t})}{s^2(s^{-1}\sqrt{g}+z\sqrt{1+2t}(s^{-1}\sqrt{g})^2)}$
(35)	$D_t(t,z)$	$1-z$	$1-4t^2$	$\frac{z(1+2t)}{g(s\sqrt{g}^{-1}+z)} = \frac{z(1+2t)}{s^2(s^{-1}\sqrt{g}+z(s^{-1}\sqrt{g})^2)}$
(55)	$C(\sigma;t,2)$	$1-\sigma$	$1-4t^2$	$\frac{8t(1-t)(1+2t)-4(\sigma+t\sigma^2+t)(1-2t^2+\sqrt{g})}{\sqrt{g}^3(s^2g^{-1}-(1+s)^2)}$
				$= \frac{8t(1-t)(1+2t)-4(\sigma+t\sigma^2+t)(1-2t^2+\sqrt{g})}{s^3(s^{-1}\sqrt{g}-(s^{-1}\sqrt{g})^3(1+s^2))}$
(119)	$C(t,q)$	$1-4t^2$	$1-q$	–

Table 2. Critical exponents.

Equation	GF	$2-\alpha_-$	$2-\alpha_+$	$2-\alpha_t$	$2-\alpha_u$	ϕ
(11)	$g(t,z)$	-1	-1	-2	-2	1
(21)	$C(t,z)$	$\frac{1}{2}$	-1	$-\frac{1}{2}$	-1	$\frac{1}{2}$
(30)	$D(t,z)$	$\frac{1}{2}$	-1	$-\frac{1}{2}$	-1	$\frac{1}{2}$
(33)	$C_t(t,z)$	$-\frac{1}{2}$	-1	-1	-2	$\frac{1}{2}$
(35)	$D_t(t,z)$	$-\frac{1}{2}$	-1	-1	-2	$\frac{1}{2}$
(55)	$C(\sigma,t,2)$	$-\frac{1}{2}$	-1	$-\frac{3}{2}$	-3	$\frac{1}{2}$
(119)	$C(t,q)$	?	-1	?	$\frac{1}{2}$	1

3.4. Limiting free energies and microcanonical densities

The partition function $Z_n(z) = \sum_{m\geqslant 0} h_n(m)z^m$ in a directed model includes objects (paths) of fixed size, but arbitrary energy m. This is the *canonical ensemble*. The *grand canonical ensemble* would include objects of arbitrary size; in our case this would be represented by the generating function $G(t,z) = \sum_{n\geqslant 0, m\geqslant 0} h_n(m)z^m t^n$. Most of the results obtained in section 2 were obtained by studying the generating function, and therefore by taking a grand canonical approach to the problem. In contrast, one may also work in the *microcanonical* ensemble: in this case a model of objects of fixed size and fixed energy is studied.

Let $h_n(\lfloor \epsilon n \rfloor)$ be the number of paths of length n and with energy $\lfloor \epsilon n \rfloor$. Then ϵ is the *density* of the energy as a fraction of n. It is not immediately clear what relation this has to the canonical ensemble and to the limiting free energy, but the connection is established by defining the (microcanonical) *density function* by

$$\mathcal{P}(\epsilon) = \lim_{n\to\infty} [h_n(\lfloor \epsilon n \rfloor)]^{1/n} \tag{163}$$

if this limit exists (see reference [35] for details about this). Generally, existence of the limiting free energy implies a weaker result.

Theorem. *Suppose that $h_n(m)$ satisfies the following assumptions:*

- *There exists a constant $K > 0$ such that $0 \leqslant h_n(m) \leqslant K^n$ for each value of n and of m.*
- *There exists a finite constant $C > 0$, and non-negative integers A_n and B_n, such that $0 \leqslant A_n \leqslant B_n \leqslant Cn$, and $h_n(m) > 0$ if $A_n \leqslant m \leqslant B_n$.*

In addition, suppose that the limiting free energy $\mathcal{F}(z) = \lim_{n\to\infty} \frac{1}{n} \log \sum_m h_n(m) z^m$ exists and is finite in $(0, \infty)$, and that it is a convex function of $\log z$. If $\mathcal{F}(z) \geqslant \max\{\epsilon_m \log z, \epsilon_M \log z\}$, then the density function $\mathcal{P}(\epsilon)$ exists in (ϵ_n, ϵ_M), and it is defined by

$$\log \mathcal{P}(\epsilon) = \lim_{n\to\infty} \frac{1}{n} \log [h_n(\lfloor \epsilon n \rfloor + \sigma_n)] \tag{164}$$

where $\langle \sigma_n \rangle$ is a sequence of integers such that $\sigma_n = o(n)$. Moreover, $\mathcal{P}(\epsilon)$ is finite and concave in (ϵ_m, ϵ_M) and the integers $\delta_n = \lfloor \epsilon n \rfloor + \sigma_n$ may be chosen as the least values of m that maximizes $h_n(m) z^m$.

Proof. Define δ_n to be the least value of m, and dependent on z, such that $h_n(m) z^m$ is a maximum. Then $A_n \leqslant \delta_n \leqslant B_n$, and

$$h_n(\delta_n) z^{\delta_n} \leqslant \sum_{m=A_n}^{B_n} h_n(m) z^m = Z_n(x) \leqslant (1 + B_n - A_n) h_n(\delta_n) z^{\delta_n}. \tag{165}$$

Take logarithms, divide by n and let $n \to \infty$. This shows that

$$\mathcal{F}(z) = \lim_{n\to\infty} \frac{1}{n} \log[h_n(\delta_n) z^{\delta_n}]. \tag{166}$$

Choose an ϵ and multiply equation (165) by $z^{-\lfloor \epsilon n \rfloor}$. Taking logarithms, dividing by n and taking $n \to \infty$ then shows that

$$\mathcal{F}(z) - \epsilon \log z = \lim_{n\to\infty} \frac{1}{n} \log[h_n(\delta_n) z^{\delta_n - \lfloor \epsilon n \rfloor}]. \tag{167}$$

But observe that $\mathcal{F}(z) \geqslant \max\{\epsilon_m \log z, \epsilon_M \log z\}$ and that $\mathcal{F}(z)$ is convex in $\log z$. Thus, if $\epsilon \in (\epsilon_m, \epsilon_M)$, then the infimum over z on the left-hand side of equation (167) is realized at a finite $z = z_1$. In other words, the right-hand side of equation (165) is finite at $z = z_1$, and this is only possible if $\delta_n - \lfloor \epsilon n \rfloor = \sigma_n = o(n)$. This shows that the limit $\log \mathcal{P}(\epsilon) = \lim_{n\to\infty} \frac{1}{n} \log[h_n(\lfloor \epsilon n \rfloor + \sigma_n)]$ exists, and completes the proof. □

In other words, existence of the free energy implies that the density function may be defined by

$$\log \mathcal{P}(\epsilon) = \inf_{z \geqslant 0} \{\mathcal{F}(z) - \epsilon \log z\}. \tag{168}$$

On the other hand, it was observed above that $\mathcal{F}(z) = \lim_{n\to\infty} \frac{1}{n} \log[h_n(\delta_n) z^{\delta_n}]$, where $\delta_n = \lfloor \epsilon n \rfloor + \sigma_n$ is that value of the energy m that maximizes $h_n(m) z^m$. Hence,

$$\mathcal{F}(z) = \sup_{\epsilon} \{\log \mathcal{P}(\epsilon) + \epsilon \log z\} \tag{169}$$

where $\epsilon \in (\epsilon_m, \epsilon_M)$. The density functions may be computed for the models discussed in section 2. Those are listed in table 3.

The logarithm of the density function $\log \mathcal{P}(\epsilon)$ is concave and continuous in (ϵ_m, ϵ_M). Jump discontinuities at ϵ_m and ϵ_M may indicate transition at zero or infinite z, while finite right and left derivatives of $\mathcal{P}(\epsilon)$ correspond to phase transitions in asymmetric models. For example, it can be shown that the critical point in an asymmetric model with density function

Table 3. Density functions.

Model	Free energy	Density function	(ϵ_m, ϵ_M)
$g_0(t, z)$ (10)	$\mathcal{F}(z) = \log z$	$\frac{1}{\epsilon^\epsilon (1-\epsilon)^{1-\epsilon}}$	[0, 1]
$g(t, z)$ (13)	$\mathcal{F}(z) = \begin{cases} 0 & \text{if} \quad z \leqslant 1/2 \\ \log 2 + \log z & \text{if} \quad z > 1/2 \end{cases}$	2^ϵ	[0, 1]
$C(t, z)$ (25)	$\mathcal{F}(z) = \begin{cases} \log 2 & \text{if} \quad z \leqslant 2 \\ \log z - \frac{1}{2}\log(z-1) & \text{if} \quad z > 2 \end{cases}$	$\frac{2(1-\epsilon)^{1-\epsilon}}{2^\epsilon (1-2\epsilon)^{1/2-\epsilon}}$	(0, 1/2]
$C_t(t, z)$ (34)	$\mathcal{F}(z) = \begin{cases} \log 2 & \text{if} \quad z \leqslant 2 \\ \log z - \frac{1}{2}\log(z-1) & \text{if} \quad z > 2 \end{cases}$	$\frac{2(1-\epsilon)^{1-\epsilon}}{2^\epsilon (1-2\epsilon)^{1/2-\epsilon}}$	(0, 1/2]
$D_t(t, z)$ (37)	$\mathcal{F}(z) = \begin{cases} \log 2 & \text{if} \quad z \leqslant 1 \\ \log(2z) - \frac{1}{2}\log(2z-1) & \text{if} \quad z > 1 \end{cases}$	$\frac{2(1-\epsilon)^{1-\epsilon}}{(1-2\epsilon)^{1/2-\epsilon}}$	[0, 1/2]
$C(s; t, 2)$ (55)	$\mathcal{F}(z) = \begin{cases} \log 2 & \text{if} \quad s \leqslant 1 \\ \log(s+1) - \frac{1}{2}\log(s) & \text{if} \quad s > 1 \end{cases}$	$\frac{2}{(1-2\epsilon)^{1/2-\epsilon}(1+2\epsilon)^{1/2+\epsilon}}$	[0, 1/2]
$G_{co}(t, 1, a; \xi)$ (83)	$\mathcal{F}(1, a; \xi) = \begin{cases} \log 2 & \text{if} \quad a \leqslant 1 \\ \log \frac{\sqrt{2}a}{\sqrt{(a-1)\sqrt{2a-1}}} & \text{if} \quad a > 1 \end{cases}$	$\frac{\sqrt{2}(2-3\epsilon+\sqrt{\epsilon^2-2\epsilon+2})}{(1-4\epsilon)^{1/4-\epsilon}\sqrt{5-3\epsilon+5\sqrt{\epsilon^2-2\epsilon+2}}}$	[0, 1/4]
$C(t, q)$ (122)	$\mathcal{F}(t) = \begin{cases} 0 & \text{if} \quad t \leqslant 1/2 \\ ? & \text{if} \quad t > 1/2 \end{cases}$	?	[0, 1]

with a finite right derivative at ϵ is located at

$$\log z_c = -\left[\frac{\mathrm{d}^+}{\mathrm{d}\epsilon} \log \mathcal{P}(\epsilon)\right]_{\epsilon=\epsilon_m}. \tag{170}$$

Discontinuities in the derivative of $\mathcal{P}(\epsilon)$ otherwise also correspond to critical points. See [35] for more details.

4. Collapse (and adsorption) in a model of colonnades

The adsorption transition discussed in section 2.2 is driven by an interaction between vertices in the paths and a wall or an interface. This transition is due to a one-body interaction involving one vertex in the path for every interaction. A two-body interaction can be introduced by an activity conjugate to pairs of vertices that are close to one another in the lattice. This interaction cannot be introduced in the (fully) directed lattice paths considered in section 2, but studied in models of partially directed paths [9] and also in models of the self-avoiding walk [40]. In those models it drives a *collapse transition* [14]; the path goes from an extended object (often considered for modelling a polymer in a good solvent), to a compact phase through a θ-transition [16], as the strength of the activity is increased. The transition to compact objects may be considered a model of polymers coming out of solution. θ conditions are encountered at the critical point separating the good solvent regime and the poor solvent regime.

A two-body interaction is introduced by defining *contacts* as a pair of vertices in a partially directed path that are also adjacent in the lattice. Any conformation of the path will have a number of contacts; this will be its energy and the activity y will be conjugate to the number of contacts. Directed square lattice paths do not admit any contacts, so that a partially directed

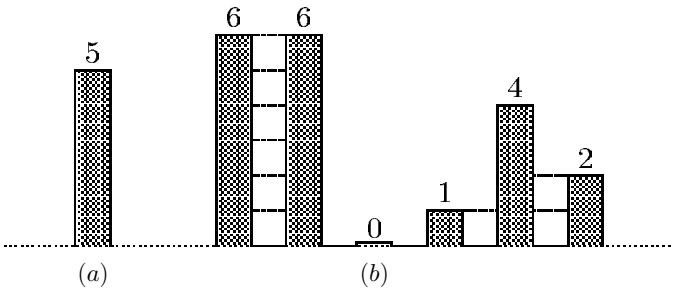

Figure 13. (*a*) A column of height 5 and length 11 steps. This column is a partially directed path that steps 5 steps in the *Y*-direction, followed by 1 step in the *X*-direction, and then 5 steps in the $-Y$-direction. (*b*) A set of interacting columns. *Contacts* between columns are two-body interactions between vertices in adjacent columns, these are denoted by dashed lines. A column of height 0 is a *visit*. The total area of a column is the shaded part, and its perimeter is the total length of the partially directed path that forms its upper boundary. A set of adjacent and interacting columns is a *colonnade*.

path model will instead be introduced to model collapse. A simplified model is discussed next [36].

4.1. A model of collapsing colonnades

A *column* of height n is a path in the square lattice (XY-plane) with starting point in the X-axis, n steps in the Y-direction, then one step in the X-direction followed by n steps in the $-Y$-direction to terminate in the X-axis. The perimeter of the column consists of $2n+1$ edges, and it encloses an area of n unit squares. Two columns are adjacent if they are separated by one step in the X-direction, and joined by an edges in the X-axis. A column and a collection of adjacent columns are illustrated in figure 13.

A set of adjacent columns on the X-axis is a *colonnade*. An interacting colonnade may be defined by introducing a two-body interaction between adjacent columns in the colonnade. A *contact* between two colonnades is a pair of vertices in adjacent columns that are adjacent in the lattice. A model of collapsing colonnades is defined by introducing activities conjugate to contacts (y), and conjugate to the width (defined as the number of columns) of the colonnade (η). The total perimeter length of the colonnade will be generated by t, and q will be the total area of the colonnade included within its columns.

Observe that the total area α of a colonnade, and its width ω (number of columns), is related to its total length ℓ by $\ell = 2\alpha + 2\omega - 1$. Thus, specifying width and area also specifies length. Hence, ignore the length generating variable t, and consider the generating function $G(q, y, \eta)$ of colonnades with area generating variable q, width generating variable η and contact generating variable y. It is possible to solve for $G(q, y, \eta)$ by finding a functional recursion using the decomposition method, as in section 2.2.

A colonnade may be *inflated* by raising the height of each column by one. This construction generates a factor of qy for each column other than the last column, and a factor of q for the last column, since a new contact is generated on the right-hand side of each column except the last, and the area of every column increases by one step. Thus, inflated colonnades are generated by $y^{-1}G(q, y, qy\eta)$. The decomposition is illustrated in figure 14.

To simplify notation, let $G(\eta) \equiv G(q, y, \eta)$. The decomposition in figure 14 shows that

$$\begin{aligned} G(\eta) &= \eta + y^{-1}G(qy\eta) + \eta G(\eta) + y^{-1}\eta G(qy\eta) + y^{-1}\eta G(qy\eta)G(\eta) \\ &= \eta + \eta(\eta + q) + \eta(\eta + q)^2 + \cdots \end{aligned}$$

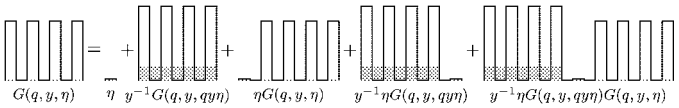

Figure 14. A functional recursion for the generating function $G(q, y, \eta)$ may be obtained using the above decomposition. A colonnade is composed either of a single column of height 0, or it is an inflated colonnade, or it is a colonnade with first column of height 0, or it is an inflated colonnade followed by a column of height 0, or finally it is an inflated colonnade, followed by a column of height 0, and then followed by an arbitrary colonnade.

This is a non-linear functional recursion, and it may be written as

$$G(qy\eta)G(\eta) + \frac{1+\eta}{\eta}G(qy\eta) + \frac{y(\eta-1)}{\eta}G(\eta) + y = 0. \tag{171}$$

An explicit expression can be obtained if $qy = 1$ by solving for $G(\eta)|_{qy=1}$ from equation (171): this gives

$$G(\eta)|_{qy=1} = \frac{1-\eta-q-q\eta-\sqrt{(1-q)((1-\eta)^2-q(1+\eta)^2)}}{2q\eta}. \tag{172}$$

There are branch points singularities in $G(q, y, \eta)|_{qy=1}$ whenever $q = 1$, or $q = (1-\eta)^2/(1+\eta)^2 < 1$. Thus, along the hyperbola $qy = 1$, the radius of convergence is given by $q_c(\eta) = \min\{1, (1-\eta)^2/(1+\eta)^2\} = (1-\eta)^2/(1+\eta)^2$ for $\eta \in [0, 1]$.

The full generating function can also be determined by solving the functional recursion in equation (171). Linearize this equation by the ansatz

$$G(\eta) = \frac{B}{\eta}\frac{H(qy\eta)}{H(\eta)} - \frac{\eta+1}{\eta}. \tag{173}$$

Substition followed by simplification gives

$$B^2H(q^2y^2\eta) + (y(\eta-1) - (\eta+1))BH(qy\eta) + yH(\eta) = 0. \tag{174}$$

This may be simplified to the linear second-order recursion with constant coefficients:

$$\alpha_2 H(q^2y^2\eta) + \alpha_1 H(qy\eta) + \alpha_0 H(\eta) + \eta H(qy\eta) = 0. \tag{175}$$

where the α_i are given by

$$\alpha_2 = \frac{B}{y-1} \qquad \alpha_1 = -\frac{y+1}{y-1} \qquad \alpha_0 = \frac{y}{B(y-1)}. \tag{176}$$

The functional recursion as in equation (175) has solution given by

$$H(\eta) = \sum_{n=0}^{\infty} \frac{(-\eta)^n (qy)^{\binom{n}{2}}}{\prod_{m=0}^{n} \Lambda((qy)^m)} \qquad \text{where} \quad \Lambda(t) = \alpha_0 + \alpha_1 t + \alpha_2 t^2 \tag{177}$$

provided that $\alpha_0 + \alpha_1 + \alpha_2 = 0$; this may be checked by direct substitution. B should be chosen so that $\sum_i \alpha_i = 0$; this occurs when

$$B = 1 \quad \text{or} \quad B = y. \tag{178}$$

The correct choice for B would give the correct solution for $G(\eta)$, and may be obtained by expanding $G(\eta)$ for small η. It follows that

$$\Lambda(t) = \frac{y}{B(y-1)}(1-t)\left(1 - \frac{B^2}{y}t\right). \tag{179}$$

Therefore

$$\prod_{m=1}^{n} \Lambda((qy)^m) = \left(\frac{y}{B(y-1)}\right)^n (qy;qy)_n (B^2q, qy)_n. \tag{180}$$

A q-deformed Bessel function is defined by

$$J(q;p,t) = \sum_{n=0}^{\infty} \frac{(-t)^n q^{\binom{n}{2}}}{(q;q)_n (p;q)_n}. \tag{181}$$

Comparison with $H(\eta)$ shows that

$$H(\eta) = J\left(qy; B^2q, \frac{\eta(y-1)B}{y}\right) \tag{182}$$

$$H(qy\eta) = J(qy; B^2q, q\eta(y-1)B). \tag{183}$$

The solution for the generating function is then given by

$$G(q,y,\eta) = \frac{B}{\eta} \frac{J(qy; B^2q, q\eta(y-1)B)}{J\left(qy; B^2q, \frac{\eta(y-1)B}{y}\right)} - \frac{\eta+1}{\eta}. \tag{184}$$

Since $J(p,q,t) = 1 + \cdots$, the term in $1/\eta$ is cancelled only if $B = 1$, so that this choice for B fixes the generating function. Thus, one finally obtains

$$1 + G(q,y,\eta) = \frac{1}{\eta}\left(\frac{J(qy; q, q\eta(y-1))}{J\left(qy; q, \frac{\eta(y-1)}{y}\right)} - 1\right). \tag{185}$$

The generating function $G_1(q,y,\eta)$ of an inflated colonnade (with no visits) can be directly be determined from equation (185). It was observed that $G(\eta) = yG_1(\eta/qy)$, where $G(\eta) \equiv G(q,y,\eta)$, since reducing the height of each inflated colonnade counted by $G_1(\eta)$ by 1 gives a unique colonnade. Hence, $G_1(\eta) = y^{-1}G(qy\eta)$, so that

$$1 + yG_1(q,y,\eta) = \frac{1}{qy\eta}\left(\frac{J(qy; q, q^2\eta y(y-1))}{J(qy; q, q\eta(y-1)} - 1\right). \tag{186}$$

$G_1(q,y,\eta) \equiv G_1(\eta)$ also satisfies the following functional recursion:

$$yG_1(\eta) = G_1(qy\eta) + (1 + yG_1(\eta))qy\eta(1 + G_1(qy\eta)) \tag{187}$$

This recursion was obtained in the study of directed vesicle models, and, in particular, in an area–perimeter model of bargraphs or histogram polyominoes [2, 3]. Let $qy \to q$ and then $\eta \to q/y$ and $y \to 1/t$ to obtain the same functional recursion as in equation (3.11) in the paper by Prellberg and Brak [53].

4.2. The phase diagram of collapsing colonnades

There is a line of essential singularities in $G(q,y,\eta)$ along the hyperbola $qy = 1$. The restriction of $G(q,y,\eta)$ to the curve $qy = 1$ is analytic along a part of $qy = 1$. If $y = 1$, then the generating function can be determined from $G_1(q,1,\eta)$. In this case

$$G_1(q,1,\eta) = \sum_{n=1}^{\infty}\sum_{k=1}^{n} A_n(k)\eta^k q^n \tag{188}$$

where $A_n(k)$ is the number of colonnades with k columns, each of height at least 1, and of total area n. Now,

$$A_n(k) = \binom{n-1}{k-1} \tag{189}$$

and direct calculation gives

$$G_1(q, 1, \eta) = \frac{q\eta}{1 - q(1+\eta)} = q\eta + q^2\eta + q^2\eta^2 + q^3\eta + \cdots. \tag{190}$$

An inflated colonnade can be deflated by taking $\eta \to \eta/qy$; this shows that

$$G(q, 1, \eta) = G_1(\eta/q) = \frac{\eta}{1 - (q+\eta)} \qquad \text{if} \quad y = 1. \tag{191}$$

There is a simple pole in $G(q, 1, \eta)$ at $q = 1 - \eta < 1$, and if $1 > \eta > 0$ then the radius of convergence of $G(q, y, \eta)$ is not determined by the curve $qy = 1$, but by a curve of simple poles $q_c(y)$ lying below the curve $qy = 1$ in the qy-plane.

Singularities of $G(q, y, \eta)$ below $qy = 1$ should be due to the roots of $H(\eta)$ in equation (173).[5] $H(\eta)$ decreases from 1 to $-\infty$ as q increases from 0 to $\min(1, y^{-1})$. Since $H(\eta)$ is continuous, there is a $q_c(y)$ where $H(\eta) = 0$ (by the intermediate value theorem). Moreover, $\frac{\partial H(\eta)}{\partial q} < 0$, so this pole is simple. This proves the presence of a simple pole in $G(q, y, \eta)$ at $q_c(y)$ for each $y \leqslant 1$. Assume that these simple poles all lie on the curve $q_c(y)$. This curve is also non-increasing with y and it should meet $qy = 1$ in the tricritical point (q_c, y_c). The obvious candidate for this point is a critical point along $qy = 1$. This may be guessed by looking at equation (172). Since the point $(q, y) = (1, 1)$ is ruled out by the above, it appears that the tricritical point is at

$$(q_c(y_c), y_c) = ((1-\eta)^2/(1+\eta)^2, (1+\eta)^2/(1-\eta)^2). \tag{192}$$

Further investigation can be done by considering the analyticity of $G(q, y, \eta)$ in the region given by $qy < 1$ and $y \geqslant y_c$. If $G(q, y, \eta)$ is analytic in this region, then this proves that the critical curve is given by $q_c = 1/y$ for $y \geqslant y_c$. Since $q_c(y) < 1/y$ for at least $y = 1$, this shows that there is a non-analyticity in $q_c(y)$ and therefore in $\mathcal{F}(y)$; this corresponds presumably to the collapse transition. Proceed by dividing equation (175) by $H(qy\eta)$ to obtain

$$\alpha_2 \frac{H(q^2y^2\eta)}{H(qy\eta)} + (\alpha_1 + \eta) + \alpha_0 \frac{H(\eta)}{H(qy\eta)} = 0. \tag{193}$$

Put $g(\eta) = H(qy\eta)/H(\eta)$, then it follows from equation (173) that

$$G(q, y, \eta) = \frac{1}{\eta}(g(\eta) - 1) - 1. \tag{194}$$

To see that the curve $qy = 1$ is a locus of essential singularities in $G(q, y, \eta)$, argue as follows. Both $H(\eta)$ and $H(qy\eta)$ have $qy = 1$ as an accumulation point of poles. If these poles do not cancel in $g(\eta)$, then they would create an essential singularity at $qy = 1$. Otherwise, assume that they do cancel. Singularities in $g(\eta)$ are then due to zeroes of $H(\eta)$. This denominator has roots between pairs of adjacent poles given by solutions of $(q; qy)_n = 0$ and $(qy; qy)_n = 0$ for $n = 1, 2, 3, \ldots$. Since $H(\eta) \neq H(qy\eta)$ if $y \geqslant y_c$ and $qy < 1$, these roots should form singularities in $g(\eta)$ that accumulate on the curve $qy = 1$. Lastly, to see that $G(q, y, \eta)$ is analytic in the region $qy \leqslant 1$ and $y > y_c$, substitute $g(\eta)$ in equation (193) to obtain

$$g(\eta) = \frac{-\alpha_0}{\alpha_1 + \eta + \alpha_2 g(qy\eta)}. \tag{195}$$

Replace α_i in this expression by the definitions in equation (176) (with $B = 1$), and define $\epsilon_p = 1 + y + (qy)^p\eta(1 - y)$ to simplify it to

$$g(\eta) = \frac{y}{\epsilon_0\left(1 - \frac{g(qy\eta)}{\epsilon_0}\right)}. \tag{196}$$

[5] $H(\eta)$ is absolutely convergent if $q < 1$ and $qy < 1$. Thus, if both $q < 1$ and $qy < 1$, then $H(\eta)$ is an analytic function, and $G(\eta)$ is a meromorphic function in the domain $q < 1$ and $qy < 1$ (it is the ratio of two holomorphic functions). Here, its singularities are given by the zeros of $H(\eta)$.

This can be developed into an infinite fraction:

$$g(\eta) = \cfrac{y}{\epsilon_0\left(1 - \cfrac{y}{\epsilon_0\epsilon_1\left(1-\cfrac{y}{\epsilon_1\epsilon_2\left(1-\cfrac{y}{\epsilon_2\epsilon_3(1-\cdots)}\right)}\right)}\right)} \tag{197}$$

with the result that an infinite fraction representation for $G(q, y, \eta)$ is obtained. Applying Worpitsky's theorem [63] shows that this is convergent whenever

$$\left|\frac{yq}{\epsilon_p\epsilon_{p+1}}\right| \leqslant \frac{1}{4} \qquad \text{for all} \quad p \geqslant 0. \tag{198}$$

Substitution of ϵ_p gives explicitly

$$\left|\frac{yq}{(1+y+(qy)^p\eta(1-y))(1+y+(qy)^{p+1}\eta(1-y))}\right| \leqslant \frac{1}{4}. \tag{199}$$

If $y > 1$ and $qy \leqslant 1$ then this implies that $G(q, y, \eta)$ is convergent for all values of y that satisfies

$$(1+y+\eta(1+y))^2 \geqslant 4y. \tag{200}$$

Solving for y, and since $y > 1$, gives

$$y \geqslant \left(\frac{1+\eta}{1-\eta}\right)^2 = y_c. \tag{201}$$

as observed in equation (192). In other words, this proves that the critical point has to occur as some value of y less or equal to $((1+\eta)/(1-\eta))^2$. The coincidence of this point with a critical point on the curve $qy = 1$ in equation (172) proves that the critical point is located here. Since the restriction of $G(q, y, \eta)$ to $qy = 1$ is analytic along $qy = 1$ for all $y > y_c$, it follows that $q_c(y) = 1/y$ for all $y \geqslant y_c$.

4.3. Scaling of collapsing colonnades

In the last two sections evidence were presented that the critical curve $q_c(y)$ of collapsing colonnades are composed of a curve of essential singularities along $qy = 1$ for $y > y_c$, and a curve of simpler singularities (poles) along $q_c(y) < 1/y$ if $y < y_c$. The critical point at (q_c, y_c) is a tricritical point, and if the free energy of this model is defined by $\mathcal{F} = -\log q_c(y)$, then it is apparent that

$$\mathcal{F}(y) = \begin{cases} > \log y & \text{if} \quad y < y_c \\ = \log y & \text{if} \quad y \geqslant y_c. \end{cases} \tag{202}$$

The scaling of the generating function can be determined by using known results for the asymptotics of q-deformed Bessel functions [52]. This will also show that collapsing colonnades are closely related to models of inflating vesicles; one such relationship was already pointed out by noting that inflated colonnades and bargraph polyominoes have the same functional recursion in equation (187). Here, the scaling of $G(q, y, \eta)$ will be seen to be similar to that of area–perimeter generating function of staircase polygons [53].

Suppose that q generates area, t vertical edges, and η horizontal edges (or width) in a model of staircase polygons. Then the generating function is given by [7, 53]

$$G_s(q, t, \eta) = \eta\left(\frac{J(q\eta, q, q^2t)}{J(q\eta, q, qt)} - 1\right). \tag{203}$$

This can be transformed into equation $G(q, y, \eta)$ in equation (185) by taking $\eta \to y$ followed by $t \to \eta(y-1)/(qy)$. This generating function is known to have the following *uniform* asymptotic behaviour [52]: For $0 < \eta, t < 1, 0 < q < 1$ define

$$z = (1 + \eta - t)/2 \qquad d = z^2 - \eta. \tag{204}$$

Define α by

$$\begin{aligned}\tfrac{4}{3}\alpha^{3/2} = {} & \log(z + \sqrt{d}) \log(1 - z + \sqrt{d}) - \log(z - \sqrt{d}) \log(1 - z - \sqrt{d}) + \mathcal{L}i_2(z - \sqrt{d}) \\ & + \mathcal{L}i_2(1 - z - \sqrt{d}) + \mathcal{L}i_2(z + \sqrt{d}) + \mathcal{L}i_2(1 - z + \sqrt{d}).\end{aligned} \tag{205}$$

Then it follows that

$$\begin{aligned}G_s(q, t, \eta) = {} & \frac{1}{2}\left(1 - t - \eta + \alpha^{-1/2}(-\log q)^{1/3} \frac{Ai'(\alpha(-\log q)^{-2/3})}{Ai(\alpha(-\log q)^{-2/3})} \sqrt{(1 - t - \eta)^2 - 4t\eta}\right) \\ & \times (1 + O(-\log q)).\end{aligned} \tag{206}$$

$Ai(x)$ is the Airy function. Comparison with equations (140) and (141) shows that $\phi = 2/3$, $2 - \alpha = 1/3$ and $2 - \alpha_u = 1/2$.

In the special case that $t = \eta$ (that is, horizontal edges and vertical edges in the staircase polygons are the same) it follows from the square root factor in equation (206) that the critical point is at $(q_c, t_c) = (1, 1/4)$. The asymptotic behaviour in the vicinity of this point is given by

$$G_s(q, t, t) \sim \frac{1}{2} - t + 4^{-2/3}(-\log q)^{1/3} \left[\frac{Ai'(4^{4/3}(1/4 - t)(-\log q)^{-2/3}}{Ai(4^{4/3}(1/4 - t)(-\log q)^{-2/3}}\right]. \tag{207}$$

One may identify the scaling fields $(1/4 - t)$ and $-\log q = -\log(1 + q - 1) \approx (1 - q)$, and in this case comparison with equations (140) and (141) shows again that this model has the exponents listed in the last paragraph. In fact, these exponents are encountered in a variety of vesicle models [53], and they are known as 'vesicle exponents'. The line $q = 1$ is again a line of essential singularities in this model, and this intersects a curve of branch points at the tricritical point.

These results are directly applicable to the colonnades generating function $G(q, y, \eta)$ in equation (185). The ratio of q-deformed Bessel functions in equation (185) can be turned into those in equation (203) by first replacing q by $q\eta$, then putting $y = 1/\eta$, and finally eliminating y by t through $qt = \eta(y - 1)/y = \eta^2(y - 1)$. In other words, the full scaling of $G(q, y, \eta)$ is given by equation (206) with the appropriate changes. This model has vesicle exponents, and a scaling function that is a ratio of the derivative of an Airy function and an Airy function. Since α is not an important contributor to the scaling behaviour, only q and the square root factor in equation (206) have to be determined to find the scaling fields. Appropriate substitutions shows that up to analytic corrections,

$$G(q, y, \eta) \sim (-\log(q/\eta))^{-1/3} \sqrt{(1 - 1/y)^2(1 - \eta)^2 - 4\eta(1 - 1/y)/y}\, F(\alpha(-\log(q\eta))^{-2/3}) \tag{208}$$

where $F(\cdot) = Ai'(\cdot)/Ai(\cdot)$ is the scaling function.

5. Conclusion

In this review the methods and general theory of directed lattice path models of linear polymers were presented. In particular, I presented Dyck path models in a variety of ensembles. The

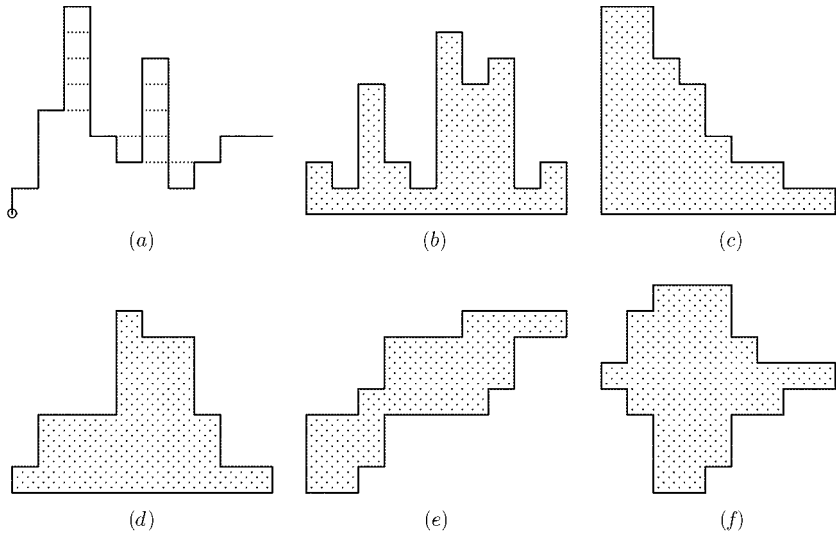

Figure 15. Directed models of walks and polygons. (*a*) Partially directed paths are more general models of collapsing and adsorbing polygons (contacts between nearest neighbour vertices are denoted by dashed lines). Dyck paths have also been generalized to Motzkin paths (in the triangular lattice). (*b*) Histogram polygons are related to partially directed paths (the upper boundary of the polygon is a partially directed path with endpoints in the X-axis. (*c*) Partition polygons, (*d*) stack polygons, (*e*) staircase polygons and (*f*) convex polygons are directed models of vesicles.

generating functions were obtained, with particular emphasis on the most common methods for deriving them. In particular, decomposition methods, the Temperley method, and a constant term formulation were presented. In each case a different model was studied.

The generating functions are expected to be subject to tricritical scaling, and the general theory of tricritical scaling, in the context of the models here, were reviewed in section 3. In section 4 a model of colonnades was investigated. This model is very closely related to models of vesicles, including staircase polygons, histogram polygons, and other models of convex or directed vesicles encountered in the literature. In particular, the generating function of colonnades may be expressed as the ratio of two q-deformed Bessel functions, and the generating functions of staircase polygons and histogram polygons are similarly ratios of q-deformed Bessel functions [53, 12]. The asymptotics of q-deformed Bessel functions was worked out by Prellberg [52], with the result that such asymptotics are also known for the model of colonnades. In many of the Dyck path models in section 2 the tricritical scaling assumptions can be tested in the generating function, and these are tabled in table 3.

In figure 15 I present some related models of directed paths and vesicles. Motzkin path [18] and partially directed path models (figure 15(*a*) [50, 64, 38]) of adsorbing polymers have also received attention in the literature. The adsorbing Motzkin path generating function is given by

$$M(t,z) = \frac{z}{1 - tz(1 - tM(t,1))} \tag{209}$$

from which one may first solve for $M(t,1)$ and then for $M(t,z)$. The upper boundary of the polygon in figure 15(*b*) is a partially directed path constrained to visit vertices only on or above the X-axis, and have endpoints in the X-axis. These are *bargraph paths*, and they can

be turned into models of adsorbing bargraph paths by weighing visits by vertices in X-axis by z. In that case the generating function is

$$B(t,z) = \frac{tz^2(1+t(1+tz)B(t,1))}{1-tz(1+t^2zB(t,1)}. \tag{210}$$

It is similarly possible to define models with weighted *edges* in the X-axis [38]. In these bargraph path models, exchange relations analogous to equation (22) have also been determined, and the adsorption of coloured models of Motzkin and partially directed paths have been studied [38]. The adsorption of periodic models of coloured partially directed paths was considered in [45] as well.

The collapse transition of a partially directed walk, with *contacts* (dotted lines in figure 15(a)) weighted by y, was also considered in [9]. The generating function of this model contains a ratio of q-deformed Bessel functions,

$$G_s(t,y) = \frac{2t - t^2(2+t-ty)H(t,y)}{t^2(1+t+y-ty)H(t,y) - 2t} \tag{211}$$

where

$$H(t,y) = \frac{J(ty,t,t^2(y-1))}{J(ty,t,t^3y(y-1))}. \tag{212}$$

Critical exponents in the tricritical framework is known for this model [9], and the scaling forms are related to that of collonades. A model of bargraph polygons in the perimeter–area ensemble is equivalent to the collonades in section 4.1, see equations (186) and (187) [2, 3, 53, 5].

The remaining directed vesicle models in figure 15 are somewhat simpler. Partition polygons in figure 15(c) are counted by q-exponentials (equation (118)) in a height–area ensemble, and in the area–perimeter ensemble by

$$P(t,q) = \sum_{n=0}^{\infty} \frac{t^{2n+2}q^n}{(t^2q;q)_n} \tag{213}$$

where q is the area generating variable. Stack polygons (figure 15(d)) [66] are closely related to partition polygons, and have generating function

$$S(t,q) = \sum_{n=0}^{\infty} \frac{t^{2n+2}q^n(1-t^2q^n)}{(t^2q;q)_n^2}. \tag{214}$$

Models of spiral walks in the square lattice are also closely related to partition and stack polygons [43, 28]. Staircase polygons (figure 15(e)) have been famously counted in the area–perimeter ensemble by Polyà [51] using Gaussian binomial coefficients. This generating function can also be derived by a functional recursion and is a ratio of q-deformed Bessel functions:

$$G_s(t,q) = t^2\left[\frac{J(q,t^2q,t^2q^2)}{J(q,t^2q,t^2q)} - 1\right] \tag{215}$$

and this is also related to collonades, when the above is compared with equation (185). Other convex polygon models, such as fully convex polygons (figure 15(f)) or partially convex polygons, have also received attention in the literature, see for example [17, 7, 12, 53, 20]. Directed animal models of adsorbing and collapsing branch polymers have also been considered [37].

There is much scope for further work in this field. More general models can be studied, and the critical behaviour in models with three or more parameters have not been described. For

example, scaling close to the triple point in figure 6 should be investigated. The description of inflating Dyck paths with an adsorbing activity in section 2.7.1 also deserves more attention, as do coloured Dyck paths and partially directed path models of adsorbing and collapsing copolymers.

Acknowledgment

EJJvR is supported by a grant from NSERC (Canada).

Appendix. Free energy and self-averaging in quenched models of coloured Dyck paths

A.1. The growth constant of adsorbing Dyck paths

The number of Dyck paths of length $2n$ is given by Catalan's number C_n. It may be checked that $C_n C_m \leqslant C_{n+m}$, and an easy proof of this inequality follows from a simple construction (called *concatenation*) on Dyck paths: Translate a Dyck path of length $2m$ so that its initial vertex coincides with the final vertex of a Dyck path of length $2n$. This produces a Dyck path of length $2(n+m)$, and note also that each pair of Dyck paths of lengths $2n$ and $2m$ gives a unique path of length $2(n+m)$ when concatenated in this way. Since there are C_n choices for the path of length $2n$, and C_m choices for the path of length $2m$, the inequality follows.

In addition to the submultiplicative inequality $C_n C_m \leqslant C_{n+m}$, it is the case that $C_n \leqslant 4^n$. This is seen by noting that two steps can be added in four ways to the endpoint of a directed path. Together, the submultiplicative inequality and the upper bound implies the existence of the limit [29–31, 65].

$$\mu_D = \lim_{n\to\infty} C_n^{1/2n} \tag{216}$$

and since the radius of convergence of $C(t)$ in equation (19) is $t_c = 1/4$, it follows that $\mu_D = 2$. The number μ_D is the *growth constant* of Dyck paths, and it is the asymptotic number of ways a step can be added while a Dyck path is generated. The numerical value of μ_D shows that Dyck paths wander away from the main diagonal in the asymptotic limit, and return with probability zero to intersect a vertex in it.

The concatenation above may be instead applied to Dyck paths with visits. In particular, if $c_{2n}(v)$ is the number of Dyck paths with v visits and half-length n, then

$$\sum_w c_{2n}(w) c_{2m}(v-w) \leqslant c_{2(n+m)}(v). \tag{217}$$

Multiplying by z^v and summing over v then shows that the partition function satisfies a submultiplicative inequality:

$$Z_{2n}(z) Z_{2m}(z) \leqslant Z_{2(n+m)}(z). \tag{218}$$

Since $Z_{2n}(z) \leqslant C_n z^n$, the result is the existence of a growth constant $\mu_D(z)$ given by

$$\mu_D(z) = \lim_{n\to\infty} [Z_{2n}(z)]^{1/2n} = \mathrm{e}^{-\mathcal{F}(z)} \tag{219}$$

where $\mathcal{F}(z)$ is the limiting free energy density of adsorbing Dyck paths per edge (unit length), given by equation (25). Thus,

$$\mu_D(z) = \begin{cases} 2 & \text{if} \quad z \leqslant 2 \\ \frac{z}{\sqrt{z-1}} & \text{if} \quad z > 2. \end{cases} \tag{220}$$

and one notices that $\mu_D(z) = 1/t_c(z)$ in equation (24).

A.2. A most popular argument

Consider now instead the number $c_n(v, [h_1h_2])$ of directed paths, above the main diagonal in the square lattice, with v visits to the main diagonal, of length n, and with initial vertex a height h_1, and final vertex a height h_2, above the main diagonal. It is possible to concatenate paths counted by $c_n(w, [hh])$ with paths counted by $c_m(v-w, [hh])$ to obtain the submultiplicative inequality[6]

$$\sum_w c_n(w, [hh])c_m(v-w, [hh]) \leqslant c_{n+m}(v, [hh]). \tag{221}$$

As above, one may multiply this by z^v, define the partition function $Z_n(z, [hh])$, and sum over v to obtain

$$Z_n(z, [hh])Z_m(z, [hh]) \leqslant Z_{n+m}(z, [hh]). \tag{222}$$

Clearly, the partition function of Dyck paths is given by $Z_n(z) = Z_n(z, [00])$, since the endpoints are fixed in the main diagonal in that case.

For any given fixed z, there are *most popular values* of $[hh]$, denoted by $[h^*h^*]$, and with h^* possibly dependent on n, so that

$$Z_n(z, [hh]) \leqslant Z_n(z, [h^*h^*]). \tag{223}$$

It follows that

$$Z_n(z) = Z_n(z, [00]) \leqslant Z_n(z, [h^*h^*]) \tag{224}$$

and by sandwiching p paths generated by $Z_n(z, [h^*h^*])$ between paths from $Z_n(z, [0h^*])$ and $Z_n(z, [h^*0])$, one finds that

$$Z_n(z, [0h^*])[Z_n(z, [h^*h^*])]^p Z_n(z, [h^*0]) \leqslant Z_{n(p+2)}(z, [00]) = Z_{n(p+2)}(z). \tag{225}$$

Take logarithms of this, divide by $n(p+2)$ and let $p \to \infty$. This shows that by equations (224) and (219),

$$\frac{1}{n}\log Z_n(z) \leqslant \frac{1}{n}\log Z_n(z, [h^*h^*]) \leqslant \mathcal{F}(z). \tag{226}$$

In other words, if one takes $n \to \infty$ above, then

$$\mathcal{F}(z) = \lim_{n\to\infty} \frac{1}{n}\log Z_n(z, [h^*h^*]). \tag{227}$$

Lastly, the most popular choice $[h^*h^*]$ may still not maximize $Z_n(z, [hh])$; the maximum over $[hh]$ for fixed n and z may occur at conformations with heights $[h_1^*h_2^*]$, where h_1^* may not be equal to h_2^*. In that case, the constructions for equations (221) and (222) give

$$\begin{aligned}(Z_n(z, [h^*h^*]))^2 &\leqslant Z_n(z, [h_1^*h_s^*])Z_n(z, [h_2^*h_1^*]) \\ &= (Z_n(z, [h_1^*h_2^*]))^2 \leqslant Z_{2n}(z, [h_1^*h_1^*]) \leqslant Z_{2n}(z, [h^*h^*])\end{aligned} \tag{228}$$

where $[h_1^*h_2^*]$ are the most popular values of $[h_1h_2]$ in $Z_n(z, [h_1h_2])$. Taking logarithms, dividing by $2n$ and taking $n \to \infty$ shows that

$$\mathcal{F}(z) = \lim_{n\to\infty} \frac{1}{n}\log Z_n(z, [h_1^*h_2^*]). \tag{229}$$

[6] The parity of $[h_1h_2]$ present a slight problem here. If both h_1 and h_2 are odd, or both are even, then n should only be even in $c_n(w, [h_1h_2])$, and otherwise n should be odd. Without further reference to this problem, the parity of $[h_1h_2]$ will be taken to fix the length of the paths as odd or even in the expressions that follow.

A.3. Self-averaging in adsorbing coloured Dyck paths

Arguments analogous to those above may be used to prove that this model is self-averaging. Let $Z_n(z, [h_1 h_2]|\chi)$ be the partition function of a model of adsorbing Dyck paths, odd labeled vertices coloured by $\chi = (\chi_1, \chi_2, \ldots)$ where χ_i is takes values in the set of colours $\{A, B, C, \ldots\}$, and with endpoints at heights $[h_1 h_2]$ above the main diagonal. Assume that visits of colour A (these are A-visits) are weighted by a, and that other visits are not weighted. While this model may seem very simplified, the results below can be (without too much difficulty) applied to more general models.

Fix $2n = Nm + r, 0 \leqslant r < m$, and let χ_0 be a sequence of colours. Consider a path P counted by the partition function $Z_{2n}(a|\chi_0) = Z_{2n}(z, [00]|\chi_0)$ of Dyck paths coloured by χ_0 and of half-length n. P may be cut into N pieces of length $m-2$ (where m is even) by deleting N vertices in P (the mth, $2m$th, etc.) and a remainder of length $r-1$. This is cut the sequence χ_0 into $\{\chi^{(1)}, \chi^{(2)}, \chi^{(3)}, \ldots, \chi^{(N)}, \chi^{(N+1)}\}$, each subsequence of length $m/2$. The endpoints of each piece of the divided P have a certain height above the main diagonal, suppose that the ℓth piece have endpoints of heights $[h_\ell, k_\ell]$. Observe that $k_{\ell-1} = h_\ell$ for $\ell = 2, 3, \ldots, N = 1$. By selecting most popular values of $[h_\ell k_\ell]$, this shows that

$$Z_{2n}(a, [00]|\chi_0) \leqslant \prod_{\ell=1}^{N} [Z_{m-2}(a, [h_\ell^*, k_\ell^*]|\chi^{(\ell)})] Z_{r-1}(a, [h_{N+1} k_{N+1}]|\chi^{(N+1)}). \tag{230}$$

Take logarithms, divide by n, and take the lim sup of the left-hand side as $n \to \infty$, but with m fixed. Then $N \to \infty$, and r varies between 0 and $m-1$. The result is that

$$\limsup_{n\to\infty} \frac{1}{2n} \log Z_{2n}(a, [00]|\chi_0) \leqslant \lim_{N\to\infty} \frac{1}{N} \sum_{\ell=1}^{N} \frac{1}{m} \log Z_{m-2}\left(a, [h_\ell^* k_\ell^*]|\chi^{(\ell)}\right). \tag{231}$$

The strong law of large numbers shows that the right-hand side approaches the average over all colourings for almost every sequence χ_0. Thus

$$\limsup_{n\to\infty} \frac{1}{2n} \log Z_{2n}(a, [00]|\chi_0) \leqslant \left\langle \frac{1}{m} \log Z_{m-2}(z, [h_\chi^* k_\chi^*]|\chi) \right\rangle_\chi \qquad \text{for almost every } \chi. \tag{232}$$

The heights $[h_\chi^* k_\chi^*]$ are the most popular heights for every colouring χ. This inequality is the first half of a proof that this model is self-averaging.

On the other hand, consider concatenating paths by translating one path so that its last vertex is two steps from the first vertex of the second path. By adding two edges in the obvious way, the paths are joined into one. If these paths are selected from the partition functions $Z_{m-2}(a, [00]|\chi^{(\ell)})$ for $\ell = 1, 2, \ldots$. Then, if $\chi_0 = \chi^{(1)}\chi^{(2)}\chi^{(3)}\ldots$, this shows that

$$\left[\prod_{\ell=1}^{N} Z_{m-2}(z, [00]|\chi^{(\ell)})\right] Z_{r-1}(a, [00]|\chi^{(N+1)}) \leqslant Z_{2n}(a, [00]|\chi_0). \tag{233}$$

Take logarithms, divide by $2n$, and take the lim inf on the right-hand side while m is fixed. Then $N \to \infty$, while r is bounded. Again applying the strong law of large numbers,

$$\left\langle \frac{1}{m} \log Z_{m-2}(a, [00]|\chi) \right\rangle_\chi \leqslant \liminf_{n\to\infty} \frac{1}{2n} \log Z_{2n}(a, [00]|\chi_0). \tag{234}$$

Our proof would be complete if we can show

$$\limsup_{m\to\infty} \frac{1}{m} \langle \log Z_{m-2}(a, [h_\chi^* k_\chi^*]|\chi)\rangle_\chi \leqslant \liminf_{m\to\infty} \frac{1}{m} \langle \log Z_{m-2}(a, [00]|\chi)\rangle_\chi. \tag{235}$$

With equation (232) and (234), this would imply that the limit

$$\mathcal{F}_{qu}(a|\chi_0) = \lim_{n\to\infty} \frac{1}{2n} \log Z_{2n}(a, [00]|\chi_0) \qquad \text{exists for almost all } \chi_0. \tag{236}$$

and moreover that

$$\mathcal{F}_{qu}(a|\chi_0) = \lim_{n\to\infty} \frac{1}{2n} \langle \log Z_{2n}(a, [00]|\chi)\rangle_\chi \qquad \text{for almost all } \chi_0. \tag{237}$$

In other words, the limiting free energy of a quenched sequence is almost always (with probability 1) equal to the averaged quenched limiting free energy (one may interchange the order of the average and the limit). This property is called *self-averaging*.

It only remains to prove equation (235):

Claim.

$$\limsup_{m\to\infty} \frac{1}{m} \langle \log Z_{m-2}(a, [h^*_\chi k^*_\chi]|\chi)\rangle_\chi \leqslant \liminf_{m\to\infty} \frac{1}{m} \langle \log Z_{m-2}(a, [00]|\chi)\rangle_\chi. \tag{238}$$

Proof. Put $m - 2 = Mp + r$ and concatenate paths of length $p - 2$ and coloured by $\chi^{(\ell)}$ as before to obtain

$$Z_{p-2}\big(a, [0k_1]|\chi^{(1)}\big) \left[\prod_{\ell=2}^{M-1} Z_{p-2}(a, [h_\ell k_\ell]|\chi^{(\ell)})\right] \times Z_{p-2}(a, [h_N 0]|\chi^{(M)}) Z_{r-1}(a, [00]|\chi^{(M+1)}) \leqslant Z_{Mp+r}(a, [00]|\chi). \tag{239}$$

Here, $\chi = \chi^{(1)}\chi^{(2)}\chi^{(3)}\ldots\chi^{(N+1)}$, and $h_\ell = k_{\ell-1}$ for $\ell = 2, 3, \ldots, M$. Observe that the above also stays true if one replaces $[h_\ell k_\ell]$ by their most popular values for each sequence $\{\chi^{(\ell)}\}$. Taking logarithms, and averaging over χ shows then that (after division by $2n = Mp + r$, and after taking the lim inf of the right hand side as $n \to \infty$ with p fixed)

$$\lim_{M\to\infty} \frac{1}{Mp + r} \sum_{\ell=2}^{M-1} \langle \log Z_{p-2}(a, [h^*_\chi k^*_\chi]|\chi)\rangle_\chi \leqslant \liminf_{n\to\infty} \frac{1}{2n} \langle \log Z_{2n}(a, [00]|\chi)\rangle_\chi. \tag{240}$$

Finally, take the lim sup and $p \to \infty$ on the left-hand side, this completes the proof. □

References

[1] Banderier C and Flajolet P 2001 Basic analytic combinatorics of directed lattice paths *Theor. Comput. Sci.* **281** 37–80

[2] Bender E 1974 Convex *n*-ominoes *Discrete Math.* **8** 31–40

[3] Bousquet-Mélou M 1992 Convex polyominoes and heaps of segments *J. Phys. A: Math. Gen.* **25** 1925–34

[4] Bousquet-Mélou M and Petkovšek M 2000 Linear recurrances with constant coefficients: the multivariate case *Discrete Math.* **225** 51–75

[5] Bousquet-Mélou M and Rechnitzer A 2002 The site-perimeter of bargraphs CNRS, LaBRI Université Bordeaux, *Preprint*

[6] Brak R, Essam J M and Owczarek A L 1998 New results for directed vesicles and chains near an attractive wall *J. Stat. Phys.* **93** 155–92

[7] Brak R and Guttmann A J 1990 Exact solution of the staircase and row-convex polygon perimeter and area generating function *J. Phys. A: Math. Gen.* **23** 4581

[8] Brak R, Guttmann A J and Whittington S G 1991 On the behaviour of collapsing linear and branched polymers *J. Math. Chem.* **8** 255–67

[9] Brak R, Guttmann A J and Whittington S G 1992 A collapse transition in a directed walk model *J. Phys. A: Math. Gen.* **25** 2437–46

[10] Brak R and Owczarek A L 1995 On the analycity properties of scaling functions in models of polymer collapse *J. Phys. A: Math. Gen.* **28** 4709–25

[11] Brak R, Owczarek A L and Prellberg T 1993 A scaling theory of the collapse transition in geometric clusters of polymers and vesicles *J. Phys. A: Math. Gen.* **26** 4565–79
[12] Brak R, Owczarek A L and Prellberg T 1994 Exact scaling behaviour of partially convex vesicles *J. Stat. Phys.* **76** 1101–28
[13] De'Bell K and Lookman T 1993 Surface phase transitions in polymer systems *Rev. Mod. Phys.* **65** 87–114
[14] de Gennes P-G 1975 Collapse of a polymer chain in poor solvents *J. Phys. Lett.* **36** L55–L57
[15] de Gennes P-G 1976 Scaling theory of polymer adsorption *J. Phys.* **37** 1445–52
[16] de Gennes P-G 1979 *Scaling Concepts in Polymer Physics* (Ithaca, NY: Cornell University Press)
[17] Delest M-P 1988 Generating functions for column-convex polyominoes *J. Comb. Theory* **48** 12–31
[18] Delest M-P and Viennot X G 1984 Algebraic languages and polyominoe enumeration *Theor. Comput. Sci.* **34** 169–206
[19] des Cloisseaux J and Jannink G 1990 *Polymers in Solution: Their Modelling and Structure* (Oxford: Oxford University Press)
[20] Domocos V 1996 A combinatorial method for the enumeration of column-convex polyominoes *Discrete Math.* **152** 115–23
[21] Feller W 1968 *An Introduction to Probability Theory and Its Applications* (New York: Wiley)
[22] Flajolet P and Sedgewick R 2001 Analytic combinatorics: functional equations, rational and algebraic functions *INRIA Rapport de Recherche No. 4103*, chapter 5
[23] Flory P J 1955 Statistical thermodynamics of semi-flexible chain molecules *Proc. R. Soc.* **234** 60–73
[24] Flory P J 1969 *Statistical Mechanics of Chain Molecules* (New York: Wiley)
[25] Forgacs G, Provman V and Frisch H L 1989 Adsorption-desorption of polymer chains interacting with a surface *J. Chem. Phys.* **90** 3339–45
[26] Gessel I M 1980 A factorisation for formal Laurent series and lattice path enumeration *J. Comb. Theory* **28** 321–37
[27] Gessel I M 1986 A probabilistic method for lattice path enumeration *J. Stat. Plan. Inference* **14** 49–58
[28] Guttmann A J and Wormald N C 1984 On the number of spiral self-avoiding walks *J. Phys. A: Math. Gen.* **17** L271–L274
[29] Hammersley J M 1962 Generalization of the fundamental theorem on sub-additive functions *Math. Proc. Camb. Phil. Soc.* **58** 235–8
[30] Hammersley J M and Morton K W 1954 Poor man's Monte Carlo *J. R. Stat. Soc.* B **16** 23–38
[31] Hille E 1948 *Functional Analysis and Semi-Groups (AMS Colloq. Publ.)* vol 31 (Rhode Island: AMS)
[32] Jain S C, Tanwar V K, Dixit V, Verma S P and Samanta S B 2001 Surface order and structure studies of polymer-solid interface *Appl. Surface Sci.* **182** 350–6
[33] James E W and Whittington S G 2002 Extent of self-averaging in the statistical mechanics of finite random copolymers *J. Phys. A: Math. Gen.* **35** 3203–11
[34] Janse van Rensburg E J 1999 Adsorbing staircase walks and staircase polygons *Ann. Comb.* **3** 451–573
[35] Janse van Rensburg E J 2000 The statistical mechanics of interacting walks, polygons, animals and vesicles *Oxford Series in Mathematics and its Applications* vol 18 (Oxford: Oxford University Press)
[36] Janse van Rensburg E J 2000 Interacting columns: generating functions and scaling exponents *J. Phys. A: Math. Gen.* **33** 7541–54
[37] Janse van Rensburg E J and Rechnitzer A 2001 Adsorbing and collapsing directed animals *J. Stat. Phys.* **105** 49–91
[38] Janse van Rensburg E J and Rechnitzer A 2002 Exchange symmetries in Motzkin path and bargraph models of copolymer adsorption *Elect. J. Comb.* **R20**
[39] Lawrie I D and Sarlbach S 1984 *Tricriticality Phase Transitions and Critical Phenomena* vol 9 ed C Domb and J L Lebowitz (London: Academic) pp 65–161
[40] Madras N N and Slade G 1993 The Self-avoiding Walk (Boston: Birkhauser)
[41] Madras N N and Whittington S G 2002 Self-averaging in finite random copolymers *J. Phys. A: Math. Gen.* **35** L427–L431
[42] Martin R, Causo M S and Whittington S G 2000 Localization transition for a randomly coloured self-avoiding walk at an interface *J. Phys. A: Math. Gen.* **33** 7903–18
[43] Melzak Z A 1962 Partition functions and spiralling in the plane random walk *Can. Math. Bull.* **6** 231–7
[44] Michelletti C and Yeomans J M 1993 Adsorption transition of directed vesicles in two dimensions *J. Phys. A: Math. Gen.* **26** 5705–12
[45] Moghaddam M S, Vrbova T and Whittington S G 2000 Adsorption of periodic copolymers at a planar interface *J. Phys. A: Math. Gen.* **33** 4573–84

[46] Odlyzko A M and Wilf H S 1988 The editor's cornern: coins in a fountain *Amer. Math. Mon.* **95** 840–3
[47] Orlandini E, Tesi M C and Whittington S G 1999 A self-avoiding walk model or random copolymer adsorption *J. Phys. A: Math. Gen.* **32** 469–77
[48] Orlandini E, Tesi M C and Whittington S G 2002 Self-averaging in the statistical mechanics of some lattice models *J. Phys. A: Math. Gen.* **35** 4219–27
[49] Owczarek A L and Prellberg T 1992 Exact solution of the discrete (1 + 1)-dimensional SOS model with field and surface interactions *J. Stat. Phys.* **70** 1175–1194
[50] Owczarek A L, Prellberg T and Brak R 1993 New scaling form for the collapsed polymer phase *Phys. Rev. Lett.* **70** 951–3
[51] Poly'a G 1969 On the number of certain lattice polygons *J. Comb. Theory* **6** 102–5
[52] Prellberg T 1994 Uniform q-series asymptotics for staircase polygons *J. Phys. A: Math. Gen.* **28** 1289–1304
[53] Prellberg T and Brak R 1995 Critical exponents from nonlinear functional equations for partially directed cluster models *J. Stat. Phys.* **78** 701–730
[54] Prellberg T and Owczarek A L 1995 Stacking models of vesicles and compact clusters *J. Stat. Phys.* **80** 755–79
[55] Privman V, Forgacs G and Frisch H L 1988 New solvable model of polymer chains adsorbing at a surface *Phys. Rev.* B **37** 9897–9900
[56] Privman V and Svrakić N M 1988 Difference equations in statistical mechanics I. Cluster statistics models *J. Stat. Phys.* **51** 1091–1110
[57] Rechnitzer A and Janse van Rensburg E J 2002 Exchange relations, Dyck paths and copolymer adsorption *Preprint*
[58] Richard C and Guttmann A J 2001 q-linear approximants: scaling functions for polygon models *J. Phys. A: Math. Gen.* **34** 4783–89
[59] Sun S-T, Nishio I, Swislow G and Tanaka T 1980 The coil-globule transition: radius of gyration of polystyrene in cyclohexane *J. Chem. Phys.* **73** 5971–75
[60] Stanley R P 1986 *Enumerative Combinatorics (Wadsworth and Brooks/Cole Advanced Books and Software)* (Belmont, CA: Wadsworth and Brooks/Cole)
[61] Temperley H N V 1956 Combinatorial problems suggested by the statistical mechanics of domains and rubber-like molecules *Phys. Rev.* **103** 1–16
[62] Vanderzande C 1998 *Lattice Models of Polymers (Cambridge Lecture Notes in Physics)* vol 11 (Cambridge University Press: Cambridge)
[63] Wall H S 1967 *Analytic Theory of Continued Fractions* (New York: Chelsea)
[64] Whittington S G 1998 A directed walk model of copolymer adsorption *J. Phys. A: Math. Gen.* **31** 3769–75
[65] Wilker J B and Whittington S G 1979 Extension of a theorem on super-multiplicative functions *J. Phys. A: Math. Gen.* **12** L245–L247
[66] Wright M E 1968 Stacks *Q. J. Math.* **19** 313–20
[67] You S and Janse van Rensburg E J 2000 A lattice tree model of branched copolymer adsorption *J. Phys. A: Math. Gen.* **33** 1171–86